Review

Bismuth-Based Z-Scheme Heterojunction Photocatalysts for Remediation of Contaminated Water

Tadesse Lemma Wakjira, Abebe Belay Gemta,* Gashaw Beyene Kassahun, Dinsefa Mensur Andoshe, and Kumneger Tadele

Read Online

ACCESS | ░░ Metrics & More | ▣ Article Recommendations

ABSTRACT: Agricultural runoff, fuel spillages, urbanization, hospitalization, and industrialization are some of the serious problems currently facing the world. In particular, byproducts that are hazardous to the ecosystem have the potential to mix with water used for drinking. Over the last three decades, various techniques, including biodegradation, advanced oxidation processes (AOPs), (e.g., photocatalysis, photo-Fenton oxidation, Fenton-like oxidation, and electrochemical oxidation process adsorption), filtration, and adsorption techniques, have been developed to remove hazardous byproducts. Among those, AOPs, photocatalysis has received special attention from the scientific community because of its unusual properties at the nanoscale and its layered structure. Recently, bismuth based semiconductor (BBSc) photocatalysts have played an important role in solving global energy demand and environmental pollution problems. In particular, bismuth-based Z-scheme heterojunction (BBZSH) is considered the best alternative route to overhaul the limitations of single-component BBSc photocatalysts. This work aims to review recent studies on a new type of BBZSH photocatalysts for the treatment of contaminated water. The general overview of the synthesis methods, efficiency-enhancing strategies, classifications of BBSc and Z-scheme heterojunctions, the degradation mechanisms of Z- and S-schemes, and the application of BBZSH photocatalysts for the degradation of organic dyes, antibiotics, aromatics compounds, endocrine-disrupting compounds, and volatile organic compounds are reviewed. Finally, challenges and the future perspective of BBZSH photocatalysts are discussed.
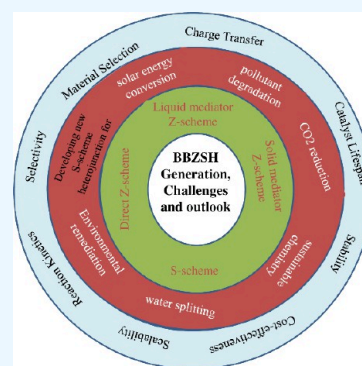
INTRODUCTION

Currently, the world faces many serious problems such as poverty, climate change, disease, pollution, energy, etc., due to the expansion of industrialization, urbanization, agricultural runoff, fuel spills, etc.[1,2] Various organic and inorganic toxins are released from different industries into the ecosystem without adequate treatment and are the main causes of surface and groundwater contamination.[3,4] In low- and middle-income countries, more than 90% of deaths are caused by water contamination.[5] Thus, pollution is not a local issue, but a planetary threat, that jeopardizes the sustainable development of modern society. Therefore, the control and prevention of water pollution require urgent global attention to have a healthy planet. So far, several techniques like filtration,[6] biodegradation,[7] physical adsorption,[8] electrochemical oxidation,[9] and advanced oxidation processes (e.g., photocatalysis, photo-Fenton oxidation, Fenton-like oxidation, etc.)[10−13] have been used to remove hazardous pollutants from wastewater. In comparison to photocatalysis, other methods have their restrictions and disadvantages. Scientists have performed a great job in creating photocatalytic technology, which has surpassed the restrictions of other techniques. Photocatalytic technology has a low cost, excellent sustainability, high

efficiency, and low environmental impact.[14] Under mild and favorable conditions, photocatalytic technology can efficiently degrade and eventually convert to nonharmful minerals.[15]

Various types of nanostructured materials such as semiconductors,[16,17] non-noble plasmonic metal,[18] metal oxides,[19,20] polymers,[21,22] composites,[23,24] etc., have been used for sunlight-based catalysis applications. Special focus has been placed on semiconductor-based photo- catalysts due to their unusual properties at the nanoscale.[25] Recently, bismuth based semiconductor (BBSc) photocatalysts have been a new emerging research topic in photocatalytic technology. The layered structures, unique physicochemical properties, visible light responsiveness, tunable band structure, etc., make this an important class of photocatalyst materials under visible light.[26−28] As a result of the hybrid orbitals of Bi 6s and O 2p in the valence band (enabling the separation of photogenerated
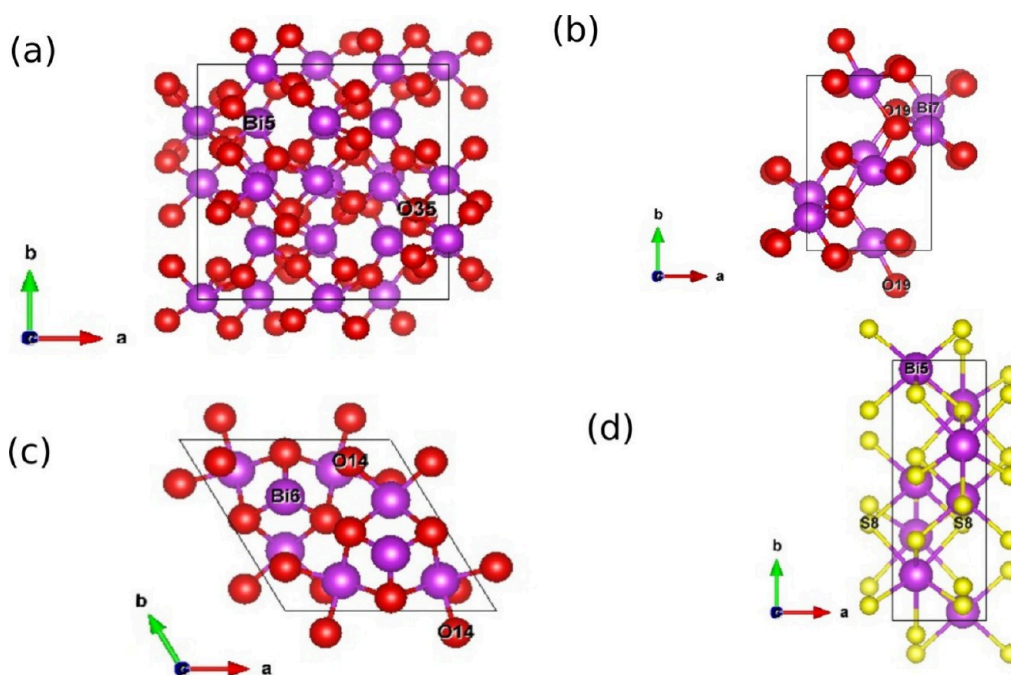
Figure 1. Crystal structure of (a) α-Bi$_2$O$_3$ phase (cubic), (b) γ-Bi$_2$O$_3$ phase (monoclinic), (c) β-Bi$_2$O$_3$ phase (hexagonal), and (d) orthorhombic phase of Bi$_2$S$_3$.

carriers), BBSc photocatalysts are better in photocatalytic activities compared to conventional photocatalysts materials such as TiO$_2$, ZnO, Fe$_2$O$_3$, etc.[29]

Moreover, bismuth metal is benign to the environment,[30] cheap and easily made, and has been found to have plasmon resonance effect properties.[31] Various compounds of BBSc photocatalysts, such as binary compounds like Bi$_2$O$_3$,[32] Bi$_2$S$_3$[33] etc., ternary compounds like Bi$_2$WO$_6$,[34] Bi$_2$MoO$_6$,[35] BiPO$_4$,[36] BiOX, BiVO$_4$,[37] etc., and multicomponent oxides such as Bi$_3$TiNbO$_9$, Bi$_4$Ti$_{0.5}$W$_{0.5}$O$_8$Cl, Bi$_4$NbO$_8$Cl, etc., have shown superior efficiency under visible light.[38] Aside from their unique properties, pristine BBSc photocatalysts have some limitations such as narrow visible light absorption, fast recombination rate of charge carriers induced by photons, small surface areas, and weak redox capacities that prevent them from being widely utilized.[39−41] A variety of methods are used, for example, elemental doping, heterojunction formation,[42,43] surface modification,[44] and noble metal decorations, to overhaul their limitations.

BBSc heterojunction improves the charge carrier separation efficiency through improved kinetics and robust redox ability. Particularly, a Z-scheme heterojunction system can improve sunlight-powered photocatalysis efficiency compared to traditional heterojunction composites. There are two benefits of the Z-scheme heterojunction photocatalyst: increased charge separation efficiency and potent redox ability.[45] As a result, isolated photogenerated electrons and holes can effectively lower the charge carriers' recombination rate. Therefore, a bismuth-based Z-scheme heterojunction (BBZSH) is considered the best alternative route to eliminate the limitations associated with a pristine BBSc photocatalyst.[31,46] Considering its benefits, several research groups have recently extensively worked on BBZSH photocatalysts for energy and environmental remediation applications.[47−53] Despite their progress in removing pollutants and antibiotics from contaminated water, Z-scheme heterojunction photocatalysts have some challenges.

For instance, material selection for both the electron donor and acceptor, designing the heterojunction architecture and optimizing the surface area and crystallinity, ensuring long-term stability and durability, and achieving high-performance photocatalysts at a large scale and reasonable cost are its challenges. The synthesis methods used to prepare photocatalytic materials have a significant impact on their photocatalytic activity. Different synthesis methods can alter the structure, morphology, composition, surface properties, and defect characteristics of the materials. These changes directly influence the materials' optical absorption, charge carrier dynamics, surface reactivity, and catalytic performance. The most common methods used to synthesize BBSc photocatalysts include solvothermal/hydrothermal methods,[54,55] coprecipitation methods,[56] sol−gel method,[21,57] solid-state thermolysis,[58] stepwise deposition techniques,[59] in situ growth,[60] and photoreduction techniques. This work aims to review the recent studies on BBZSH photocatalysts for treating contaminated water. In particular, classifications of BBSc photocatalysts, the synthesis methods, efficiency-enhancing strategies, Z-scheme and S-scheme heterojunction photocatalytic mechanisms, and the use of BBZSH photocatalysts for the elimination of harmful pollutants, antibiotics, aromatics compounds, endocrine-disrupting compounds and volatile organic compounds from water are reviewed.

■ CLASSIFICATION OF BBSC PHOTOCATALYSTS

BBSc photocatalysts are a new generation of photocatalytic material with tunable band gaps that respond to visible light. They have layered structures, resulting in interlayer electric fields (IEFs) that facilitate the separation of photogenerated charge carriers during catalysis. It is possible to classify BBSc photocatalysts according to different aspects. In terms of their chemical composition, BBSc photocatalysts can be divided into metallic bismuth, binary compounds, ternary oxides, and multicomponent oxides. Bismuth is the heaviest and one of

the pnictogens elements, with an electron configuration of $[Xe]4f^{14}5d^{10}6s^26p^3$. It exists in a natural state and has two ores namely: bismuthinite (bismuth sulfide) and bismite (bismuth oxide). Since bismuth is found regularly as a byproduct of the mining of Cu, Pd, and Sn, it is relatively inexpensive for a rare metal.[61] Bismuth and its compounds are nontoxic.[30] Hence, bismuth is considered a green metal. It has a plethora of distinct characteristics, such as being very brittle, having a low melting point, having low thermal conductivity, etc. The unusual properties at the nanoscale make metallic Bi the best photocatalyst due to its plasmonic properties,[31] and quantum confinement effect. Hence, it can be used directly in semiconductor photocatalysts or cocatalysts to speed up charge separation and hence boost photocatalytic activity.[62]

Bismuth oxide is a binary oxide of bismuth metal that exists in two forms: trivalent (Bi_2O_3) and pentavalent (Bi_2O_5). Bismuth trioxide is the most common and exists in different crystal phases, each with its unique properties and characteristics. The most commonly observed crystal phases of Bi_2O_3 are α-Bi_2O_3, β-Bi_2O_3 and γ-Bi_2O_3 as shown in Figure 1a–c. α-Bi_2O_3 is the most stable and well-known form α-Bi_2O_3 and it crystallizes in a cubic crystal structure, belonging to the space group $Pa3$. It has a high melting point and excellent stability and is commonly used in various applications, including catalysis, gas sensing, and optical devices. β-Bi_2O_3 phase of Bi_2O_3 has a hexagonal crystal structure, belonging to the space group P63/mmc. It is metastable and can be formed by high-temperature synthesis, specifically above 730 °C. It exhibits different properties compared to α-Bi_2O_3, such as improved photocatalytic activity, making it a promising material for solar energy conversion and environmental remediation.[63,64] γ-Bi_2O_3 phase is less commonly observed and is generally obtained under specific synthesis conditions. It has a monoclinic crystal structure, belonging to the space group $P2_1/c$. The Bi−O bond distances in this crystal range from 2.14 to 2.57°A.[65] It differs from the α and β phases in terms of its structural arrangement and properties. γ-Bi_2O_3 exhibits enhanced electrical conductivity and has shown potential in applications such as solid oxide fuel cells and electrochemical devices.[64] Bismuth sulfide (Bi_2S_3) is another compound of bismuth that can exist in different crystal phases. The most commonly known crystal phases of Bi_2S_3 are orthorhombic and monoclinic. Orthorhombic is the most stable and often observed phase with $Pnma$ space group. It has a layered structure, with bismuth and sulfur atoms arranged in alternating layers as plotted in Figure 2d. It is a direct bandgap semiconductor and exhibits interesting properties, such as a high absorption coefficient in the visible and

near-infrared spectral region. There are two different sites where Bi^{3+} cations are found. The first site cations are bonded to six $S^{2−}$ atoms. The lengths of the bonds between Bi and S range from 2.68 to 3.07 Å. The second cation is bonded to seven $S^{2−}$ atoms, and the bond lengths between Bi and S range from 2.60 to 3.41 Å. $S^{2−}$ atoms are also present in three different sites. The five Bi^{3+} atoms form distorted edge-sharing SBi_5 square pyramids with the first two $S^{2−}$ anions, while the third $S^{2−}$ anion binds to three Bi^{3+} atoms. These characteristics make orthorhombic a potential material for applications in optoelectronics, photovoltaics, and photocatalysis.[66] A monoclinic phase of Bi_2S_3 has a different crystal structure compared to orthorhombic. It belongs to the space group $C2/m$. It is metastable and can be obtained through specific synthesis methods or under certain conditions. This phase may exhibit properties different from those of orthorhombic, and its characterization and potential applications are still being explored.

Another class of BBSc-layered compounds is ternary oxides, and multicomponent oxides typically have Sillen, Aurivillius, and Sillen-Aurivillius phases. The best examples of a Sillen phase photocatalyst are BiOX (X= F, Cl, Br, or I) and bismuth oxide (Bi_2O_2) nanomaterial. The BiOX material is a ternary semiconductor with a unique layered structure that is made up of interwoven $[Bi_2O_2]$ and double X slabs, as shown in Figure 2. The bond between Bi−O and Bi−X is strong and covalent. In contrast, the bond between X−X is weak and due to van der Waals forces. BiOX has attracted a great deal of research interest in both experimental and computational aspects because of its small bandgap, high electron density, and strong photooxidation ability. BiOX has an indirect band gap in its bulk state, but it has a high valence band edge because of the interaction between X np orbitals and O 2p orbitals. BiOX is widely used in photocatalysis, but its ability to absorb visible light depends on the type of halogen ion present. However, Sillen structure photocatalysts have a low light absorption and fast recombination rate, which affects their efficiency for environmental remediation and energy conservation applications.

Aurivillius oxide is a layered material with a general formula of $[A_{n−1}B_nO_{3n+1}][Bi_2O_2]$, where $[A_{n−1}B_nO_{3n+1}]$ is perovskite slabs, $[Bi_2O_2]^{2+}$ is bismuth oxide slab and n is the number of octahedral layers[67] as indicated in Figure 2b. It is formed by bismuth oxide sheets swapped with one or more perovskite slabs. They can provide a suitable electronic system for visible light absorption and provide the opportunity to modify the electronic band structure by substituting the A or B sites.[68] Swedish chemist Bengt Aurivillius described this crystal structure in 1949 for the first time, which was interesting for its ferroelectric properties. The VB in this crystallographic family primarily consists of O 2p states, while the CB is predominantly comprised of Bi 6p orbitals. The optical band gap varies from 2.5 to 2.8 eV. The most well-known and studied example of the structure of the Aurivillius phase is $Bi_4Ti_3O_{12}$. Other examples include Bi_2WO_6, Bi_2MoO_6, Bi_3TiNbO_9, and Bi_2WO_6. Aurivillius oxides are ferroelectric materials and exhibit good ionic conductivity. This makes them effective in enhancing photogenerated charge separation, which is beneficial for various photocatalyzed reactions. Additionally, the small optical band gaps of specific Aurivillius structures enable them to absorb visible light efficiently.[67]

Another class of bismuth-based structures is the Sillen-Aurivillius phases, as shown in Figure 2c. These are layered oxyhalide materials with a general formula of $[A_{n−1}B_nO_{3n+1}][Bi_2O_2]_2X_m$. The number of perovskite layers is represented by
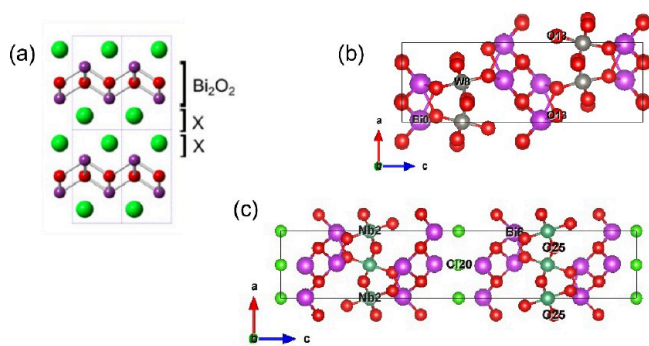
Figure 2. (a) Unit cell sillen structure of BiOX crystal, (b) unit cell aurivillius structure of Bi_2WO_6, (c) unit cell sillen-aurivillius structure of Bi_4NbO_8Cl.

n, while X represents the halide. $[Bi_2O_2]$ is fluorite, and $[A_{n-1}B_nO_{3n+1}]$ represents perovskite plates.[69,70] The number of perovskite layers is an important parameter for controlling and improving photocatalytic activity because of the wide range of cations. The dimension and composition of perovskites affect their electronic and transport properties. Recently, bismuth-based Sillen-Aurivillius structures such as Bi_4NbO_8Cl, $Bi_4Ti_{0.5}W_{0.5}O_8Cl$, $Bi_7Fe_2Ti_2O_{17}X$ (X = Cl, Br, I) have been reported for photocatalysis. Due to the small band gap, ferroelectric property, ionic conductivity, layered crystal structure, and stability, they are efficient for the degradation of organic pollutants.[70] The presence of ferroelectricity can have both direct and indirect effects on photocatalytic activity. It influences photocatalytic activity by facilitating photoinduced charge carrier separation, promoting surface charge transport, increasing photocurrent and absorption, and modifying surface reactivity. Hence, ferroelectric materials offer exciting opportunities for developing efficient and sustainable photocatalysts for various applications in energy conversion and environmental remediation. Furthermore, ionic conductivity has also a significant impact on the photocatalytic activity of a material. Higher ionic conductivity can improve the photocatalytic activity by promoting charge carrier transport, enhancing the mass transport of reactants, and facilitating electrochemical reactions.

It is also possible to classify BBSc photocatalysts based on their Z-scheme heterojunction generations. The Z-scheme heterojunction photocatalysts have evolved into four generations. They are the first-generation (liquid mediator) Z-scheme, the second-generation (solid mediator) Z-scheme, the third-generation (direct Z-scheme) and the fourth-generation (S-scheme) heterojunction. For the first time, in 1979 Bard and his colleagues reported on the concept of the Z-scheme heterojunction in the semiconductor industry using two photosystems.[71] The three elements that make up their model are semiconductor I (SC-I), semiconductor II (SC-II), and electron mediator. A model was derived from the photosynthesis mechanism in plants, in which SC-I and SC-II harvest the photon energy that is used to reduce CO_2 to carbohydrates and oxidize H_2O to O_2 with a rough quantum yield of unity. The transfer between two semiconductors is facilitated by an electron shuttle mediator as shown in Figure 3a. The most popular redox

mediators used in first-generation Z-scheme heterojunctions are IO^{-3}/I^-,[72] Fe^{3+}/Fe^{2+},[73] VO^{2+}/VO^{2+}, $[Co(bpy)_3]^{3+/2+}$ and $[Co(phen)3]^{3+/2+}$.[74] Electron shuttle mediators serve as electron acceptors and donors, separating the physical contact between the two photocatalysts. However, in the first-generation Z-scheme hetero- junction, the electron acceptor and donor are reacting with the electrons and holes generated in SC-I and II, as a result, the number of electrons and holes generated in SC-I and II decreases. Additionally, the reverse reaction and the shielding effect are other limitations of the first-generation BBZSH Photocatalysts. Thus, to conquer the drawbacks, the Tada group replaced the liquid mediator with a solid mediator in 2006, assuming that the photogenerated electron would flow smoothly between the two semiconductors and recombine across a low-contact resistance interface. They published the first study on a $CdS/Au/TiO_2$ Z-scheme ternary heterojunction for photocatalytic water splitting.[75] This year was a turning point for the development of second-generation Z-scheme heterojunction photocatalysts. Figure 3b shows the second-generation Z-scheme heterojunction. Various types of materials, such as reduced graphene oxide,[43] carbon quantum dot,[76] graphitic carbon nitride,[77] and noble metals (Au, Ag)[78,79] used as solid electron mediator. These materials act as a bridge, which serves as an electron shuttle mediator. The presence of a bridge between two photocatalysts enhances the process of separating electrons and holes generated by photons, increasing the redox capability and photocatalytic activities of the composites.[80]

Direct Z-scheme heterojunction, which describes the third-generation Z-scheme heterojunction. Direct Z-scheme systems share similar charge-transfer pathways with the first and second-generation Z-schemes but do not use a mediator as shown in Figure 3c. In direct Z-scheme heterojunctions, there is no use of media between the two photocatalysts of the photosystem. The charge carriers induced by photons are transported directly through the interface of two semiconductors, resulting in a shorter transport distance and higher photo- catalytic efficiency. This occurs when the holes in the photosystem with the least positive valence band combine with the weak electrons from the photosystem with the least negative conduction band. In this photocatalyst, an induced internal electric field participates in an oxidation and reduction reaction that separates the photo-induced pairs $e^- - h^+$ on the surface of a photosystem. Consequently, the lifespan of the $e^- - h^+$ pairs increases and maintains a superior redox capability between the photoinduced e^- in the CB of photosystem I and the holes in the VB of photosystem II. Then after the two photosystems are in contact, e^- transfers from SC-I to SC-II due to Fermi-level equilibration. This creates a positive charge in SC-I and a negative charge in SC-II. Consequently, the electron density decreases at the edges of the SC-I energy band, while accumulating at the edges of the SC-II energy band.[81] Due to these benefits, direct Z-scheme heterojunctions can effectively use photon energy by increasing the lifespan of $e^- - h^+$ and optimizing redox capacity. Hence, utilizing Z-scheme heterojunctions, one can improve the photocatalytic activity of photocatalysts by reducing $e^- - h^+$ recombination.[40,42]

The S-scheme heterojunction is a type of photocatalytic system that consists of two different semiconductors (reduction photocatalysts and oxidation photocatalysts) with staggered energy band alignments. In this configuration, one semiconductor acts as a photosensitizer, while the other acts as a catalyst. The S-scheme heterojunction improves photocatalytic activity through several mechanisms: It enables efficient charge
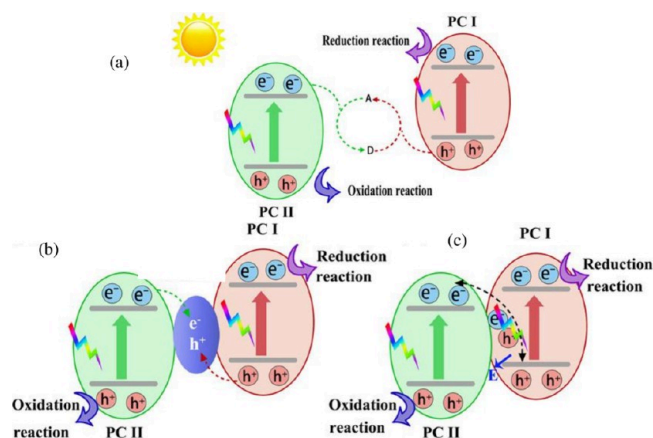
Figure 3. Schematic representation of (a) first generation, (b) second generation, and (c) third generation Z-scheme heterojunction photocatalyst. Reproduced from ref 40 under terms of the CC-BY license. Copyright 2022 The Authors.

separation, utilizes a redox potential gradient, offers synergistic effects, and broadens the spectral response. Collectively, these factors enhance the overall performance of the photocatalytic system, making the S-scheme heterojunction an effective strategy for improving photocatalytic activity.

The S- and Z-scheme heterojunctions are two different configurations of heterojunction systems commonly used in photocatalysis. Although both configurations aim to improve the efficiency and performance of photocatalytic reactions, they differ in their charge-transfer mechanisms, energy-level alignments, and redox potential gradients. The S-scheme heterojunction relies on the spatial separation of charge carriers, staggered energy band alignments, and a redox potential gradient. On the other hand, the direct Z-scheme heterojunction utilizes an interfacial electron relay mechanism, and direct energy band alignment often does not establish a significant redox potential gradient. These differences in configuration affect the efficiency and characteristics of charge transfer and overall photocatalytic activity. Furthermore, in S-scheme heterojunctions, there is a Fermi energy difference, which contributes to charge transfer between two photocatalysts. Because of the presence of an internal electric field between two photocatalysts, charge transfer in S-scheme heterojunctions facilitates more charge separation, which increases photocatalytic activity. However, there is no charge transfer due to the Fermi energy difference in a Z-scheme heterojunction.[82]

SYNTHESIS AND EFFICIENCY ENHANCING STRATEGIES OF BBSC PHOTOCATALYSTS

There are two general approaches to the preparation of photocatalytic materials, that is, top-down and bottom-up.[83] Mechanical, electrical and thermal forces are used in the top-down approach to crushing bulk materials into microparticles or nanoparticles. Due to the chemical reactions and attractive forces small molecules and atoms are assembled in bottom-up processes. Specifically, the BBSc photocatalysts can be synthesized through physical, chemical, and biological (green) methods. In contrast to physical synthesis methods, chemical synthesis methods are profoundly dependent upon chemical solvents, while green synthesis methods are characterized by nontoxic chemicals and substrates.[84] The performance of catalysts depends on various parameters such as morphological characteristics such as particle shape, size and surface area, electronic structures, catalyst dose, pH and pollutant concentration, and temperature.[76] Therefore, synthesis methods may have a significant contribution to enhancing the noninherent parameters of the photocatalytic materials, such as morphology and surface properties. To date, the BBSc photocatalyst has received special research attention in the catalysis field owing to its strong redox reaction capacity.[5,41,85] Particularly, the BBZSH photocatalysts facilitate the transfer of photogenerated charge carriers by forming more positive VB and negative CB potentials with stronger oxidation and reduction abilities. From a practical standpoint, two major difficulties in creating highly effective photocatalysts are their low quantum yield and their lack of efficiency in harvesting visible light. Several methods for synthesizing BBSc photocatalysts, such as solvothermal, hydrothermal, coprecipitation, template-assisted methods, etc., have been proposed to address these is- sues. In the next section, an overview of preparation techniques for BBSc photocatalysts is presented.

Synthesis Methods of BBSc Photocatalysts. The hydrothermal synthesis method belongs to synthesis by

chemical methods. It is the most widely reported method for the synthesis of BBSc photocatalysts. Hydrothermal syn- thesis promotes the formation of well-crystallized BBSc photocatalysts and allows for the precise control of the size, shape, and morphology. The high-pressure and high-temperature con- ditions in hydrothermal reactions lead to the controlled growth of nanoparticles, resulting in improved crystallinity and reduced defects in the material. BBSc photocatalysts synthesized using hydrothermal methods often exhibit enhanced photocatalytic activity compared to other synthesis techniques. This is attributed to the controlled crystallinity, morphology, and composition achieved through hydrothermal synthesis. These advantages make hydrothermal synthesis a valuable technique for developing efficient photocatalytic materials. Besides, hydrothermal/solvothermal synthesis methods has also dis- advantages such as requires high-temperature and high-pressure conditions, reaction time is often longer and not suitable for large-scale production due to the autoclave requirement. Recently, several types of Z-scheme heterojunction photo- catalysts, such as $In_2S_3/BiOBr$,[86] Ag_2O/Bi_2WO_6,[48] $BiVO_4/RGO/g\text{-}C_3N_4$,[87] etc., have been prepared by using the hydrothermal method. Hu et al.[86] developed a Z-scheme indium $In_2S_3/BiOBr$ heterojunction for photodegradation of organic pollutants under visible light. Li et al.[87] constructed a Z-scheme heterojunction of $BiVO_4/RGO/g\text{-}C_3N_4$ for the degradation of antibiotics. Xue et al.[88] created a double Z-scheme $g\text{-}C_3N_4/Bi_2WO_6/AgI$ photocatalyst via hydrothermal route for the degradation of organic pollutants in aqueous solutions. A direct heterojunction of Bi_2S_3 and Sb_2S_3 photo- catalysts for dye degradation and reduction was also developed using the hydrothermal method by Li et al.[53] Using a simple hydrothermal precipitation approach, a new Z-scheme flower- like Ag_2WO_4/Bi_2WO_6 photocatalyst with excellent efficiency was successfully pre- pared for the degradation of rhodamine B (RhB).[89] Furthermore, Su et al.[90] synthesized the direct Z-scheme heterojunctions of $Bi_2MoO_6/UiO\text{-}66\text{-}NH_2$ using a facile solvothermal method. The synthesized sample was tested for the degradation of antibiotics such as fluoroquinolone, ofloxacin (OFL), and ciprofloxacin (CIP) under visible light. Compared to the pristine photocatalyst, all heterojunction photocatalysts have better photocatalytic degradation efficiency due to the formation of direct Z-scheme heterojunction. A series of $BiPO_4/Bi_2MoO_6$ Z-scheme heterostructures were success- fully synthesized by a one-pot solvothermal method.[91]

A solution combustion method is a chemical synthesis method of nanostructured materials. It is an exothermic reaction mechanism in which the precursor and solvents are mixed at the molecular level to form a solid-phase product. The solution combustion method offers simplicity, cost-effectiveness, and control over composition. But it may have limitations in terms of morphology control, potential impurities, high-temperature requirements, and scalability. Recently, Hezam et al.[92] used a solution combustion method to create a direct Z-scheme heterojunction photocatalyst material composed of $Cs_2O/Bi_2O_3/ZnO$. The small energy band gap of 1.92 eV of Cs_2O was chosen to expand the range of light absorption. ZnO and Bi_2O_3 are ideal for direct Z-scheme systems because of their position between minimum conduction and maximum valence bands. The chemical bath deposition method is a chemical synthesis technique primarily used to prepare thin films of various materials from aqueous precursor solutions at temper- atures below 100 °C. Recently, Sahnesarayi et al. prepared a
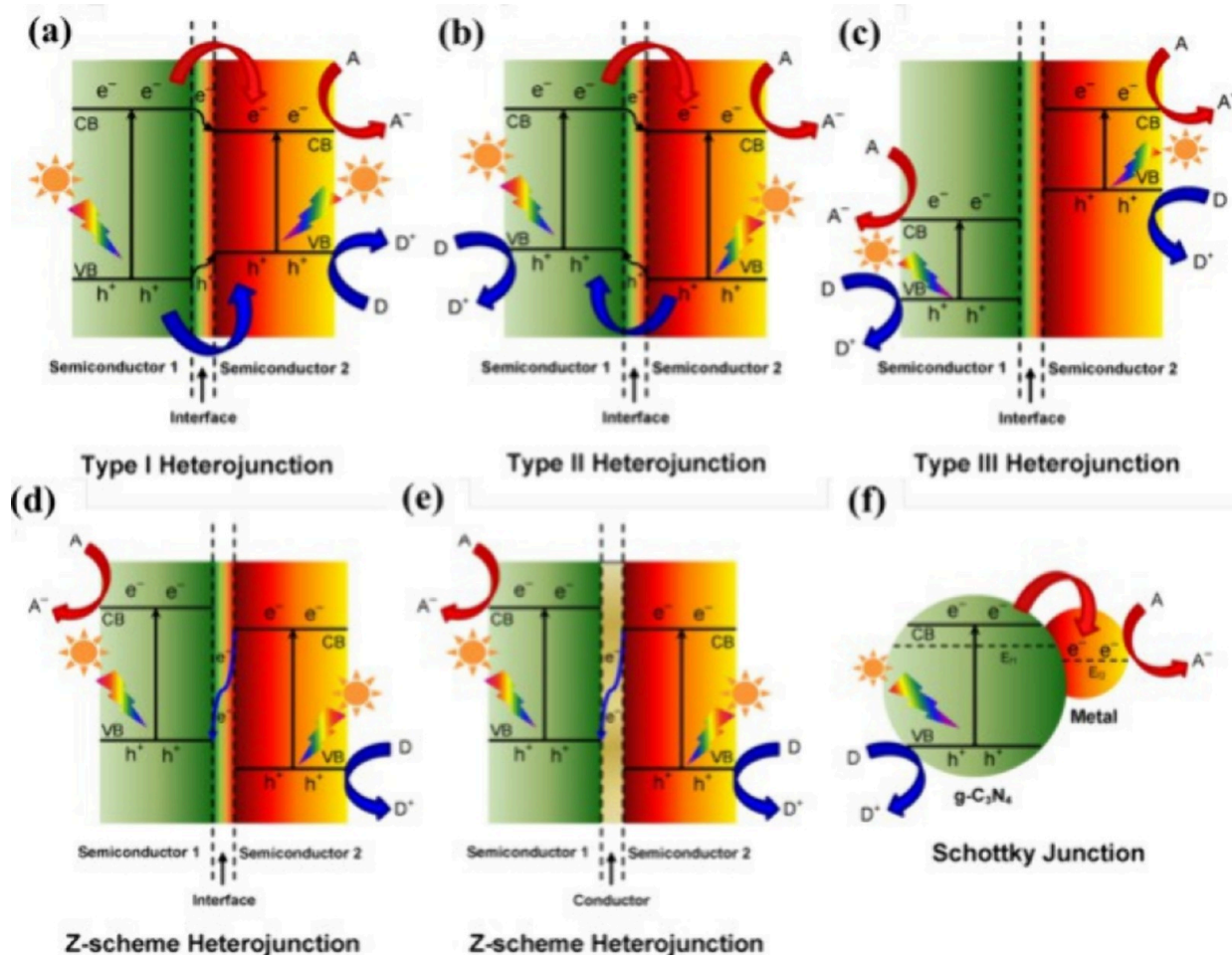
Figure 4. Physical diagram of heterojunction photocatalysts types (a), Type-I, (b), Type-II, (c), Type-III, (d, e) Z-scheme heterojunctions, and (f) Schottky junctions. Adapted in part with permission from ref 110. Copyright 2016 American Chemical Society.

photoelectrode of a Bi_2O_3 nanosheet using the chemical deposition method.[93]

The coprecipitation method is a chemical synthesis route commonly used for the preparation of inorganic and metal-based photocatalysts. The benefits of this approach include its convenient synthesis, cheapness, and low energy usage. However, its drawbacks include particle aggregation, small surface area, impurities, and uncontrolled morphology.[94] Recently, a binary Z-scheme heterojunction of $BiOI/(BiO)_2CO_3$ photocatalyst was synthesized by using the coprecipitation method for photodegradation of sulfasalazine antibiotics.[95] The ionic layer adsorption and reaction method is another chemical synthesis method commonly used to prepare uniform, large surface area thin films. In this technique, the substrate is individually submerged in a cationic and anionic solution. As an illustration, a new P−N junction of $Bi_4Ti_3O_{12}$ nanofibers−BiOI nanosheets was created by the ionic layer adsorption and reaction approach.[96] Sol−gel synthesis is another method of synthesis for BBSc photocatalysts. Sol−gel synthesis offers some advantages over other methods, such as being able to control composition, size, and morphology, mixing precursors homogeneously, and incorporating dopants and cocatalysts. However, it has the disadvantages of requiring multiple steps and longer processing times, requiring organic solvents, and being sensitive to reaction conditions. For examples, the Z-scheme heterojunction of $Bi_2O_3/CuBi_2O_4$

photocatalyst were synthesized by using sol−gel method for PMS activation and Lev degradation.[97]

In the field of nanomaterials preparation, green synthesis is a rapidly emerging technology. As a reducing and stabilizing agent, plants, bacteria, fungi, and algae are used. As a result, the green method of nanomaterials is an eco-friendly, biocompatible, cheap, and nontoxic method. Recently, a green synthesis method was used to synthesize Z-scheme heterojunction photocatalysts. For example, the Z-scheme heterojunction of CdSe/BiOCl photocatalysts was synthesized through the green synthesis method for organic dye degradation.[98] Similarly, Li et al. used the green synthesis method to prepare heterostructured ternary Cd/CdS/BiOCl photocatalysts for the removal of persistent organic contaminants in wastewater.[99]

Efficiency Enhancing Strategies. BBSc photocatalysts have gained significant attention due to their unique electronic structure and excellent photocatalytic properties.[100] Although BBSc photocatalysts show impressive photocatalytic performance, they have limitations such as weaker charge separation, poor charge carrier mobility, small surface area and high rates of recombination, low reducing ability, and limited visible-light absorption. To further enhance their efficiency, several strategies can be employed. Construction of heterojunction, band gap engineering, cocatalyst deposition, and morphology control are some key techniques to improve the photocatalytic performance of bismuth-based photocatalysts.[25] In this section, the recent

progress on BBSc photocatalyst heterojunction construction and elemental doping strategies are discussed.

Today extensive research efforts have been devoted to proposing heterojunction systems to solve the shortcomings of single-component BBSc photocatalysts. One example of improving charge separation efficiency and enhancing photocatalytic performance is by constructing Z- scheme heterojunction nanocomposites using two semiconductors. By designing a proper heterojunction-type photocatalytic system, it is possible to isolate electrons and holes in separate locations, which in turn extends the lifetime of photogenerated carriers.[71,101,102] However, the design and construction of highly active heterojunction photocatalysts remain a challenging and new focus of research. In this section, various types of heterojunctions and other related junctions are discussed.

- Type I Heterojunction: In a Type I heterojunction, the energy bands of two different semiconductor materials align in such a way that the conduction band minimum (CBM) of one semiconductor is lower than the CBM of the other semiconductor, while the valence band maximum (VBM) of the first semiconductor is higher than the VBM of the second semiconductor as shown in Figure 4a. This results in an overlapping of the energy bands at the interface. This type of heterojunction exhibits a staggered band alignment, where the CBM and VBM levels are misaligned between the two semiconductors. As a result, an electron can easily transfer from one semiconductor to the other without any energy barrier.[103,104]

- Type II Heterojunction: In a Type II heterojunction, there is a staggered alignment of energy bands as shown in Figure 4b. The CBM of one material is higher than that of the other material, while the VBM of one material is lower than that of the other material. This band offset causes photoinduced electrons and holes to be spatially separated between the two materials, facilitating efficient charge separation and promoting photocatalytic activity. Type II heterojunctions are commonly used in various photocatalytic systems.[103,104]

- Type III Heterojunction: Type III heterojunctions consist of two semiconductor materials with both the CBM and VBM of one semiconductor being higher than the respective levels of the other semiconductor as shown in Figure 4c. This leads to a discontinuity or offset between the energy bands of the two semiconductors. This type of heterojunction exhibits a broken-gap or broken-alignment band structure, where there is no overlap or misalignment of the CBM and VBM levels at the interface. Consequently, there is a significant energy barrier for carriers transferring from one semiconductor to the other.[103,104]

- P−N Junction: A P−N junction is created by connecting a p-type semiconductor to an n-type semiconductor as plotted in Figure 4f. At the interface between the p-type and n-type regions, there is a depletion region due to the diffusion of charge carriers. The P−N junction allows for efficient charge separation and can be useful in various applications, including solar cells and light-emitting diodes.[56]

- Schottky Junction: A Schottky junction is formed at the interface between a metal and a semiconductor. It creates a barrier at the interface, known as the Schottky barrier,

which affects the charge carrier transport. Schottky junctions are commonly used in electronic and optoelectronic devices due to their unique characteristics and rectifying properties.[38]

- Z-scheme and S-scheme Heterojunction: Z-scheme heterojunctions are a specific type of heterojunction design used in photocatalysis. This configuration involves two different semiconductor materials with suitable band alignments, typically referred to as photocatalysts 1 and 2 as shown in Figure 4d, e. In a Z-scheme heterojunction, photogenerated electrons in one photocatalyst (photocatalyst 1) can transfer to the conduction band of the other photocatalyst (photocatalyst 2), while photogenerated holes move in the opposite direction. This scheme typically utilizes Type II heterojunction. There is an efficient charge transfer occurs via a mediator material or a conductive bridge. The transferred electrons and holes participate in redox reactions on the respective photocatalyst surfaces, facilitating pollutant degradation or other desired photochemical transformations. Hence, the Z-scheme design enhances charge separation and provides a continuous redox cycle, resulting in efficient utilization of light energy for photocatalysis.[50] The S-scheme is the fourth generation Z-scheme heterojunction is a photocatalytic system that involves two different photocatalysts connected in a series to achieve efficient charge separation and enhance overall photocatalytic activity.[55] An S-type heterojunction design was considered to be formed by connecting two n-type semiconductors. According to Shawky and Mohamed, it is also possible to create S-scheme heterojunctions from n-type or p-type semiconductors, provided that the reduction photocatalyst must have a higher Fermi level and conduction band position than the oxidation photocatalyst.[105] In this scenario, the induced electric field plays a vital role in transferring charge carriers between the two photocatalysts. The reduction photocatalyst has a smaller work function and a higher Fermi level, while the oxidation photocatalyst has a greater work function and a lower Fermi level.[106] The performance of S-scheme heterojunction photocatalysts is influenced by several key factors such as band alignments and level matching, light absorption, charge carrier dynamics (lifetime and diffusion length of electrons and hole) and catalyst loading and its morphology.[107] Hence, understanding electronic processes is very important for photocatalytic applications. Because by studying the kinetics and pathways of electron and hole transfer, researchers can identify the key processes influencing overall photocatalytic performance and develop strategies to optimize them through mate- rial design and interface engineering.[108] Careful selection and design of materials in S-scheme systems can significantly enhance charge transfer dynamics. That is the choice of a suitable electron acceptor and donor can help optimize the charge transfer process. Furthermore, to enhance the charge kinetics in the S-scheme heterojunction, manipulation of the interfaces between different materials is crucial. It can be done by modulating surface properties using doping, codoping, and surface decorating.[109]

Most single-component BBSc photocatalysts exhibit wide band gap, limiting their absorption of visible light. Band gap

engineering techniques, such as doping with elements like nitrogen or sulfur, can narrow the band gap and extend light absorption into the visible range. By increasing the absorption of visible light, the photocatalytic efficiency can be significantly enhanced. Hence, doping is an effective technique for enhancing photocatalytic activity as it regulates the optoelectronic properties and dynamics of the materials.[111] In photocatalysts, doping is one of the primary objectives to trap photoexcited charge carriers and to promote their separation. There are two distinct types of elemental doping: metal and nonmetal doping. Metal doping can impact the electronic structure of photocatalysts in two ways. First, it introduces defects in the crystal, which increases the absorption properties of the photocatalyst and enhances the lifespan of the photogenerated charge carrier. Second, it generates a surface plasmon resonance effect on a Bi-based semiconductor surface. The presence of surface plasmon resonance (SPR) can robust the spectral response of semiconductor photocatalysts and enhance its quantum yield.[100] Noble metals such as Ag, Ni, Au, Pt, Pd, V, and others have been reported to be used to modify the electronic band structure of Bi-based semiconductor photocatalysts. These metals absorb photoinduced electrons on the surface of semiconductor materials and enhance the lifespan of photogenerated charge carriers thereby boosting photocatalytic reactions.

By introducing nonmetallic elements, energy levels can be created between the conduction and valence bands in BBSc photocatalyst photocatalysts. This leads to improved optical properties of pure BBSc photocatalysts. Furthermore, it enhances charge transmission, which promotes the effective separation of electron−hole pairs and hinders the recombination of photoinduced charge carriers. Liang et al. successfully conducted a simple hydrothermal synthesis to prepare a dual-doped Bi_2WO_6, decorated with metallic bismuth (Bi) and nonmetallic carbon (c) atoms. The synthesized material was instigated with different characterization techniques. The results showed that the codecorated C/Bi Bi_2WO_6 exhibited significantly higher photocatalytic activity than the undoped Bi_2WO_6 when decomposing various industrial pollutants under visible light, including phenol, ciprofloxacin, bisphenol A, rhodamine B, and methyl orange. The synergistic effects of SPR and C doping are attributed to the increased photocatalytic activities.[112]

Belousov et al.[113] recently conducted a comparative study on the efficacy of doping and heterojunction methods using LED light, to enhance the efficiency of Bi_2WO_6 photocatalyst. $Bi_2W_{0.5}Mo_{0.5}O_6$ and Bi_2WO_6/g-C_3N_4 composites were synthesized using solid solution and hydrothermal synthesis methods, respectively. According to the findings, the approach of adding dopants proved to be effective. The most successful result was achieved when using $Bi_2W_{0.5}Mo_{0.5}O_6$ to break down methylene blue, resulting in a conversion rate of 52.9% and a TON of 0.022. The use of only a small amount of H_2O_2 also resulted in impressive degradation rates for methylene blue (97.9% conversion, TON of 0.040) and phenol (81.2% conversion, a TON of 0.056). Another alternative in band gap engineering is the deposition of cocatalysts on the surface of BBSc, as it enhances charge carrier separation and improves the efficiency of specific reactions. Co-catalysts, such as noble metals (e.g., Pt, Au) or co- catalysts like NiO or CoO_x, can serve as active sites for charge transfer and promote specific reaction pathways. The appropriate choice and deposition of cocatalysts can accelerate the kinetics of photocatalytic reactions, leading to enhanced efficiency. The key advantages of doping on photocatalysts are (i) enhancing visible light absorption, (ii) efficient charge carrier separation, improving catalytic activity, (iv) extended lifespan and stability, and (v) impart selectivity and tunability to photocatalysts, enabling control over the types of reactions they can catalyze.

PHOTOCATALYTIC DEGRADATION MECHANISMS IN Z- AND S-SCHEME HETEROJUNCTIONS

Photocatalytic degradation relies on the use of radiation and photocatalysts to produce ROS.[40] The photocatalytic degradation mechanism in Z-scheme heterojunctions can be summarized as follows. (i) Both photocatalyst 1 and photocatalyst 2 should have suitable band gaps to absorb light in the desired range, usually in the visible or near-ultraviolet (UV) region. Photons with sufficient energy are absorbed by these materials, promoting electron transitions from the valence band to the conduction band. (ii) Upon photon absorption, both photocatalysts generate electron−hole pairs. For example, in photocatalyst 1, electrons move to the conduction band (CB1), leaving holes in the valence band (VB1). Similarly, in photocatalyst 2, electrons are excited to the conduction band (CB2), and holes are created in the valence band (VB2). (iii) The photogenerated electrons in the conduction band of photocatalyst 1 can transfer to the conduction band of photocatalyst 2 due to the formation of a suitable energy band alignment or via a conductive bridge (e.g., metal or carbon-based catalysts). This transfer occurs as a result of a suitable energy-level difference and efficient charge-transport pathways. Similarly, holes in the valence band of photocatalyst 2 can transfer to the valence band of photocatalyst 1. This hole transfer from photocatalyst 2 to photocatalyst 1 is necessary to complete the Z-scheme and create a continuous redox cycle for efficient pollution degradation. (iv) Once the photogenerated electrons and holes are separated and transferred between the two photocatalysts, they can participate in various redox reactions on the surface of the materials. Photogenerated holes in photocatalyst 1 (VB1) can oxidize adsorbed organic molecules on the surface, producing reactive oxygen species (ROS), such as hydroxyl radicals. These ROS are highly reactive and can effectively degrade the pollutants. At the same time, photogenerated electrons in photocatalyst 2 (CB2) can reduce oxygen molecules or other suitable electron acceptors, leading to the production of superoxide radicals or other reactive species that facilitate pollutant degradation. V) To increase the photocatalytic efficiency, the recombination of the photogenerated electron−hole pairs should be minimized. The appropriate band alignment and material properties of the Z-scheme heterojunction facilitate efficient charge separation and minimize electron−hole recombination. This ensures a continuous flow of charge carriers, allowing for sustained degradation of pollutants.[80,114,115]

The charge transfer mechanism in an S-scheme heterojunction can be explained as follows: When light (photons) is incident on the heterojunction, it generates electron−hole pairs in both semiconductors due to the absorption of photons. The absorption of photons leads to the excitation of electrons from the valence band to the conduction band, leaving behind holes in the valence band. The two semiconductors in the heterojunction have different energy levels, which create a barrier at the interface, called a band offset. This offset leads to a difference in the energy levels of the conduction and valence bands between the two semiconductors. Because of the band offset, the energy bands in the two semiconductors bend at the interface. In one semiconductor, the conduction band edge is higher, while in the
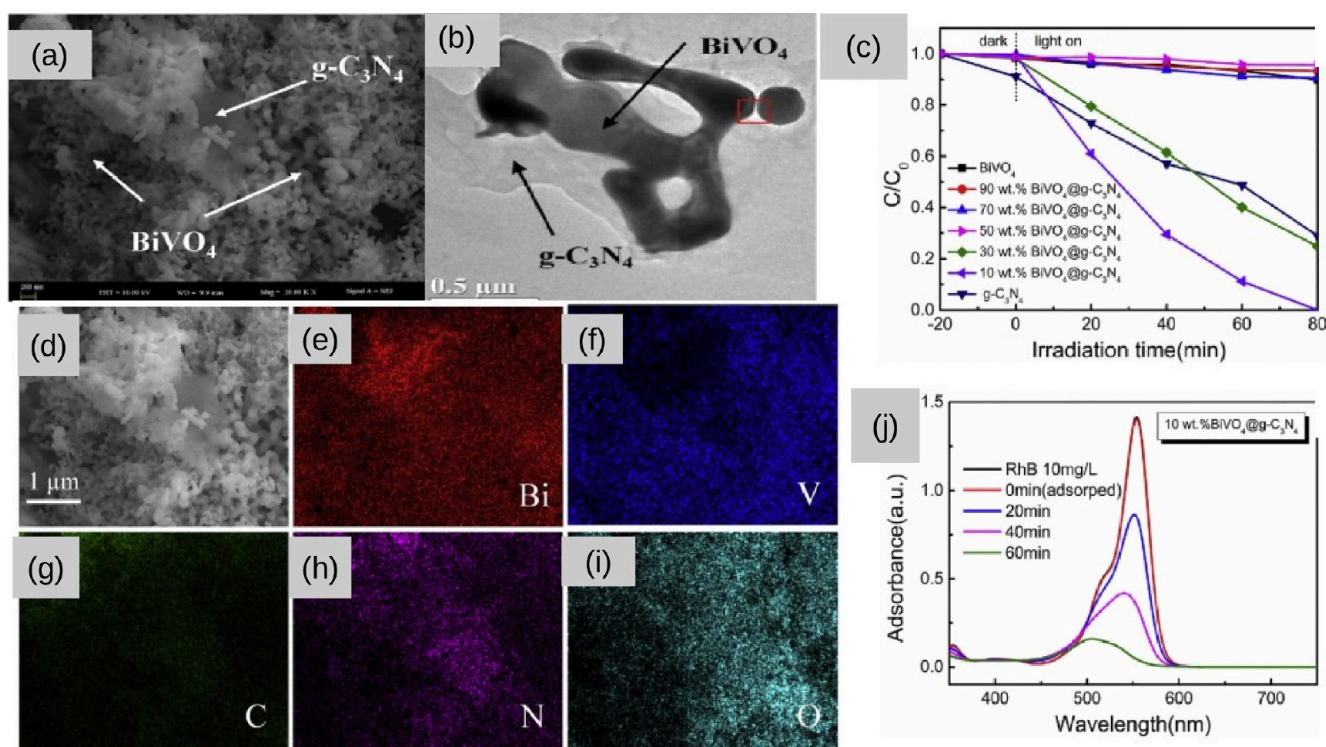
Figure 5. (a) SEM image of 10 wt % $BiVO_4$@g-C_3N_4 Z-scheme heterojunction, (b) TEM Image of 0 wt % $BiVO_4$@g-C_3N_4 Z-scheme heterojunction, (c) UV–vis diffuse reflectance spectra of the samples, (d–i) SEM elements mapping of 10 wt % $BiVO_4$@g-C_3N_4 heterojunctions and (j) UV–Vis spectra of RhB at different visible irradiation-times in the presence of 10 wt % $BiVO_4$@g-C_3N_4. Adapted in part with permission from ref 127. Copyright 2019 Elsevier.

other semiconductor, the valence band edge is higher. The photogenerated electrons in the semiconductor with a higher conduction band edge will transfer to the semiconductor with a lower conduction band edge, as electrons tend to move from higher to lower energy levels. This transfer of electrons is known as electron injection or electron transfer.[116] On the contrary, photogenerated holes in the semiconductor with a lower valence band edge will transfer to the semiconductor with a higher valence band edge, because holes tend to move from higher to lower energy levels. This transfer of holes is known as hole injection or hole transfer. The enhanced photocatalytic activity of S-scheme heterojunctions can be attributed to several underlying mechanisms. These mechanisms are related to the unique structural and electronic characteristics of S-scheme heterojunctions and their ability to facilitate efficient charge carrier separation and utilization. The efficient charge separation, cascade electron transfer, dual cocatalyst effect, interface states, and synergistic effects all contribute to the improved utilization of photoinduced charges for photocatalytic reactions, leading to higher catalytic activity and efficiency.[117,118] By understanding this general charge transfer mechanism in S-scheme heterojunctions, researchers can design and optimize these structures to enhance their efficiency in applications such as solar cells, photocatalysis, and photodetectors.

BBZSH PHOTOCATALYTIC DEGRADATION

Organic Dye Degradation. In the 21st century, due to the rapid development of industrialization, various toxic substances, such as synthetic chemicals, fertilizers, dyes, heavy metals, etc., are among the sources of water contaminants.[119] Organic dyes are mostly used to impart color to various materials, including

textiles, plastics, paper, and fabrics.[120] Approximately 7×10^5 tons of pigments and organic dyes are discharged into the environment in industrial wastewater.[121] Photocatalytic degradation using advanced catalysts offers a promising approach for the remediation and removal of organic dyes from contaminated water sources, contributing to environmental sustainability.[5,22,25,85,122] Recently, BBZSH photocatalysts have gained considerable attention for dye degradation applications due to their advanced charge transfer and separation capabilities. For instance, Mosleh et al. synthesized the Z-scheme heterojunction of Bi_2WO_6/Ag_2S/ZnS photocatalyst for degradation of methyl green (MG) and auramine-O (AO). These studies have shown that the construction of Bi-based Z-scheme heterojunctions can significantly improve the photocatalytic performance for dye degradation.[123] In another studies reported by Bi et al. Bi_2WO_6/$ZnIn_2S_4$ a double Z-scheme configuration resulted in a dye degradation efficiency that was 12–63 times higher than that of a single component photocatalyst.[124] This suggests that the incorporation of multiple semiconductors in a Z-scheme configuration can enhance the separation of charge carriers and improve the overall photocatalytic efficiency for dye degradation. Despite this, Mahalakshmi et al. also synthesized the Z-scheme Bi_2O_3/g-C_3N_4 heterojunction photocatalysts using in situ thermal polymerization method for degradation of methylene blue (MB) dye. The 1:1 ratio of Bi_2O_3/g-C_3N_4 heterojunction photocatalyst performs highest photocatalytic degradation of 91.2% after 120 min of visible-light irradiation.[125] Furthermore, the optimized composition of g-C_3N_4/$BiYWO_6$ heterojunction photocatalysts has shown significant improvement in the degradation of methylene blue under visible light exposure, indicating its potential for wastewater remediation works.[126] Furthermore, Zhong and his colleagues utilized a
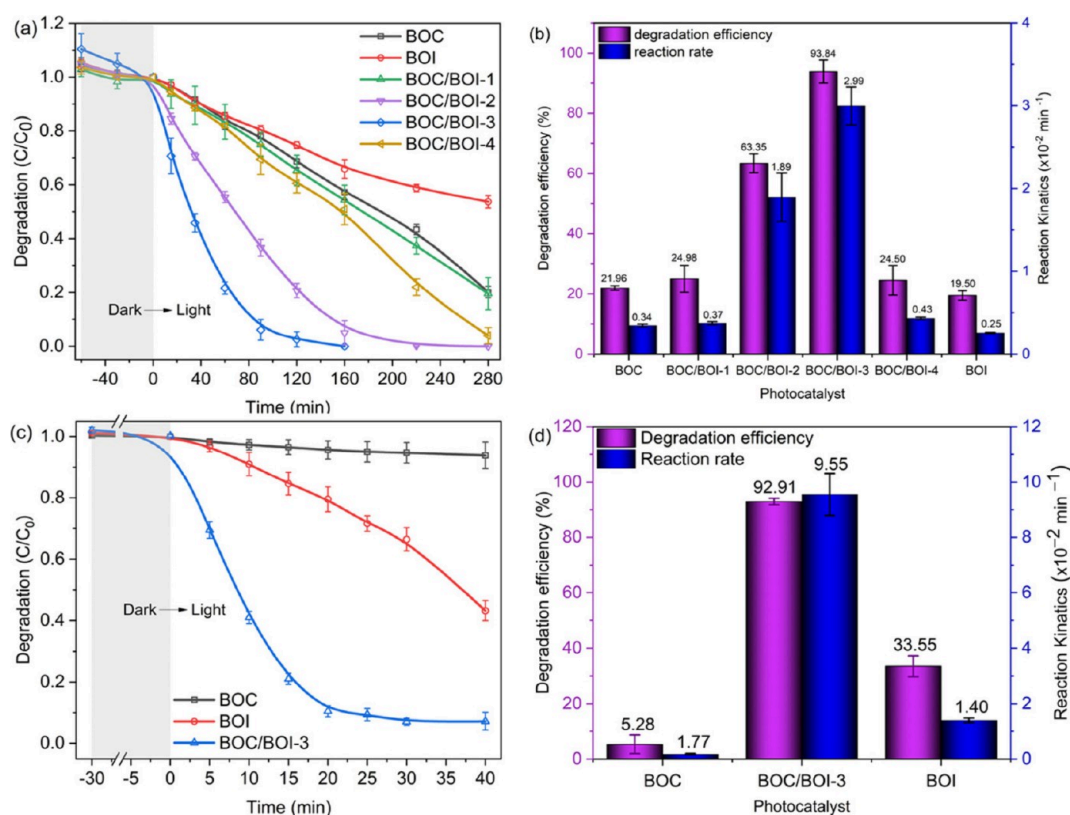
Figure 6. (a, b) RhB degradation by photocatalysis and its effectiveness with reaction rate constants applied to all samples; (c, d) BPA degradation by photocatalysis and its effectiveness with reaction rate constants applied to BOI, BOC, and BOC/BOI-3 samples. Adapted in part with permission from ref 102. Copyright 2022 The Authors.

simple hydrothermal process to synthesize heterojunction composites of $BiVO_4@g-C_3N_4(100)$. The formation of the heterojunctions was validated through various characterization techniques. Figure 5a displays the scanning electron microscopy (SEM) image. The images obtained from TEM depict (Figure 5b) a distinct interface between $BiVO_4(121)$ and $g-C_3N_4(100)$, signifying the successful formation of the heterojunction between the two materials through the hydrothermal reaction. Figure 5c, demonstrates UV−vis diffuse reflectance spectra of the samples. The EDX elemental mapping analysis (Figure 5d–i) confirmed the presence of five constituent elements, including Bi, V, O, C, and N, indicating the successful synthesis of homogeneous $BiVO_4$ and $g-C_3N_4(100)$ composite structures. Using simulated visible light to irradiate RhB, photocatalytic activity was evaluated. Based on the experimental results, the composite structure of $10\% BiVO_4@g-C_3N_4(100)$ showed the highest photocatalytic performance, with photodegradation rates 2.36 and 30.58 times greater than those for pure $g-C_3N_4$ and pure $BiVO_4$. As shown in Figure 5j, the absorption peak of RhB drastically decreased after 60 min of irradiation of the catalysts for RhB.

In another study reported by Hao et al. a ternary Z-scheme heterojunction of $WO_3/Ag_3PO_4/Bi_2WO_6$ photocatalyst was fabricated via a one-pot hydrothermal method for degradation RhB.[128] The result shows that, the Z-scheme heterojunction photocatalysts were shown an outstanding photocatalytic degradation rate constant of 1.9 and 1.3 times higher than that of pure Bi_2WO_6 and $WO_3−Bi_2WO_6$ photocatalysts, respectively. Li et al. have also synthesized Z-scheme heterojunction of $Bi_2Fe_4O_9/Bi_2WO_6Z$ photocatalysts using a facile hydrothermal method. The Z-scheme heterojunction of $Bi_2Fe_4O_9/Bi_2WO_6Z$

was able to photodegrade 100% of RhB in 90 min, demonstrating significant catalytic activity.[129] Din et al.[102] conducted a study on the Z-scheme heterojunction of the 3-dimensional hierarchical Bi_3O_4Cl/Bi_5O_7I, using calcination and solvothermal methods. Figure 6a−d shows how Bi_3O_4Cl (BOC), Bi_5O_7I (BOI), and BOC/BOI-3 photocatalyst the decomposition of BPA and RhB dye in an aqueous solution under visible light. The heterojunction of BOC/BOI-3 showed enhanced degradation efficiency of 97% and 92% for RhB and bisphenol A (BPA), respectively. The untreated photocatalysts only achieved 20% and 10% efficiency for RhB dye, respectively, and 2.3% and 37% for aqueous pollutants containing BPA, respectively. The improved efficiency of this photocatalyst is attributed to its ability to effectively absorb visible light, its large surface area, and its enhanced separation and transport of photoexcited electron−hole pairs. Furthermore, BBSc Z-scheme heterojunction photocatalysts for the removal of organic dye pollutants are summarized in Table 1. Based on several report studies,[124−126] it is evident that Bi-based Z- scheme heterojunctions hold great promise for the efficient degradation of dyes in wastewater treatment processes, offering a feasible solution to address the environmental concerns associated with dye pollution. The utilization of Bi-based Z-scheme hetero-junctions has shown great potential in the degradation of dyes, with significantly improved photocatalytic performance and higher degradation efficiency compared to single component photocatalysts.[130]

Antibiotics Degradation. Antibiotics are chemicals that are used to treat infections caused by bacteria and for livestock production. Particularly, wastewater from hospitals and pharmaceutical companies ares the primary sources of anti-

Table 1. BBZSH Photocatalysts for the Removal of Organic Dyes

S.No.	Photocatalysts	Synthesis methods	Application	Light source	Irradiation time (min)	Eff. (%)	ref.
1	g-C_3N_4/Bi_2WO_6	Hydrothermal method and heat treatment	Photodegradation of methylene blue		180	100	131
2	SnO_2/Bi_2S_3/$BiOCl$	One-spot hydrothermal	Photocatalytic degradation of rhodamine B	Visible light	180	80.8	132
3	Bi_2MoO_6@Co_3O_4	Two-step hydrothermal method	Photoanode for photo		110	88.43	41
4	Ag_2O_2/Bi_2MoO_6	Hydrothermal and coprecipitation	Photocatalytic degradation			86	133
5	g-C_3N_4@Bi/$Bi_2O_2CO_3$	Simple solvothermal method	Photocatalytic degradation of rhodamine B	visible light	120	93	101
6	Bi_2Fe_4O/$BiWO_6$	Facile hydrothermal	Photocatalytic degradation of rhodamine B		90	100	129
7	Ag/AgI/BiOI	Facile ion exchange and photoreduction	Photocatalytic degradation of methyl orange	500 W xenon lamp	180	93	134
8	Cu_2O/Au/$BiPO_4$	Hydrothermal method	Photocatalytic degradation of methyl orange	300 W xenon lamp	60	100	135
9	$KNbO_3$/Bi_2O_3	In situ growth method	Photocatalytic degradation of methyl orange	375 W mercury lamp	50	90.8	136
10	g-C_3N_4/Bi_2O_3/$BiPO_4$	Simple one-step hydrothermal process	Photocatalytic degradation of methylene orange		160	90	137
11	g-C_3N_4/Bi_4O_7	Calcination methods	Photocatalytic degradation of MB, phenol, rhodamine, bisphenol	500 W halogen lamp			138
12	CdSe/BiOCl	Green synthesis method	photodegradation of RhB 40 100 98	Ultraviolet-light	40	100	98
13	Cd/CdS/BiOCl	Green synthesis method	photodegradation of RhB	Visible light		90	99
14	$Bi_2Fe_4O_9$/Bi_2WO_6	Facile hydrothermal method	Photodegradation of RhB	Visible light	90	100	129
15	Bi2WO6/Ag_2S/ZnS	Hydrothermal method	Degradation of methyl green (MG) and auramine-O (AO) dyes	Visible light		82.75, 77.41	123
16	Bi_2WO_6/C-Dots/TiO_2	Facile chemical wet technique	Degradation of fluoroquinolone levofloxacin	Sunlight	88.3	90	139
17	$BiVO_4$/TiO_2	Hydrothermal method	RhB degradation	Visible light	74.4		140
18	TiO_2/$BiVO_4$	Sol−gel method	Degradation of azo dyes	Visible light	10	98.75	141
19	Bi2O3/MoSe2	Hydrothermal method	Degradation of methylene blue dye	Visible light	80	96.5	142

biotics.[59,60] Hence, their accumulation in the environment hurts ecosystems. The elimination of antibiotics from the environment using different techniques such as biodegradation, membrane separation, coagulation, and absorption has been re-ported. Conventional methods of contaminated treatment are inefficient at eliminating antibiotics. This is mainly because of the low biodegradability of antibiotics, which makes their removal difficult. Furthermore, some antibiotics cannot be removed using conventional treatment methods, which are expensive. However, advanced oxidation processes (AOPs) have shown promise for breaking down antibiotics into smaller, harmless, and biodegradable compounds.[143] Photocatalysis has great potential for eliminating antibiotics from aquatic environments. Bismuth oxides, which can absorb a broad range of light (approximately 780 nm), are commonly used in photocatalytic applications. Bi_4O_7 is one such oxide with a band gap of 1.99 eV. It has the potential to match the bandgap of In_2O_3 and improve the photocatalytic capability of In_2O_3 under visible light by constructing a Z-scheme heterojunction with In_2O_3.[144] A solid-state synthesis method was used to prepare the hetero-junction of In_2O_3/Bi_4O_7 for the degradation of doxycycline hydrochloride. Based on the results, doxycycline hydrochloride photodegrades 92.1% more efficiently in 2 h than pure silicon dioxide and bichromate. Bai et al. synthesized Z-scheme Bi_2S_3/$Bi_2O_2CO_3$ photocatalysts for the degradation of antibiotics and organic compounds in wastewater. The fabricated heterojunction has photocatalytic efficiency of 61% and 89% for degradation of ciprofloxacin antibiotic) and rhodamine B dye, respectively. In another studies report by Wen et al. a direct AgI/$Bi_4V_2O_{11}$ photocatalyst was synthesized using a combination of

coprecipitation and hydrothermal methods, for sulfamethazine drug photodegradation. The Z-scheme heterojunction photocatalysts have been found to be the most effective photocatalysts for sulfamethazine (SMZ) degradation, with 91.47% SMZ being degraded within 60 min.[145]

A recent study by Yin et al. introduced a Z-scheme heterojunction called MT-$BiVO_4$/P@g-C_3N_4 that was developed to degrade tetracycline hydrochloride (TC-HCl) from water.[146] In this study, the photocatalysts were composed of P-doped graphite carbon nitride nanosheets loaded with $BiVO_4$ in two coexisting phases, monoclinic scheelite (M-$BiVO_4$) and tetragonal zircon (T-$BiVO_4$). This material was abbreviated as MT-$BiVO_4$ and was produced using a hydrothermal method. Photocatalytic experiments confirmed that 5%MT−$BiVO_4$/P@g-C_3N_4 had the highest reaction rate, which was 3.8 times higher than g-C_3N_4, 1.6 times higher than that of P@g-C_3N_4, 1.9 times higher than $BiVO_4$, and 2.1 times higher than 5 of $BiVO_4$/g-C_3N_4. The improved performance was attributed to several factors, including P-doping of the modified g-C_3N_4, isotype heterojunction effects of MT-$BiVO_4$, and the Z-scheme heterojunction formed between MT-$BiVO_4$ and P@g-C_3N_4. These factors increase the absorption range of visible light and accelerate the transfer and separation of charge carriers between the catalysts. Jin et al.[57] created a Z-scheme Au@TiO_2/Bi_2WO_6 heterojunction to break down antibiotics. Bi, Ti, and Ag contribute to the plasmon resonance effect which enhances the photocatalytic activity of the heterojunction. Under visible light irradiation, the optimal mass ratio of Au@TiO_2 to Bi_2WO_6 degraded sulfamethoxazole (SMX) and tetracycline hydrochloride (TC) by 96.9% and 95.0% within 75 min, respectively.
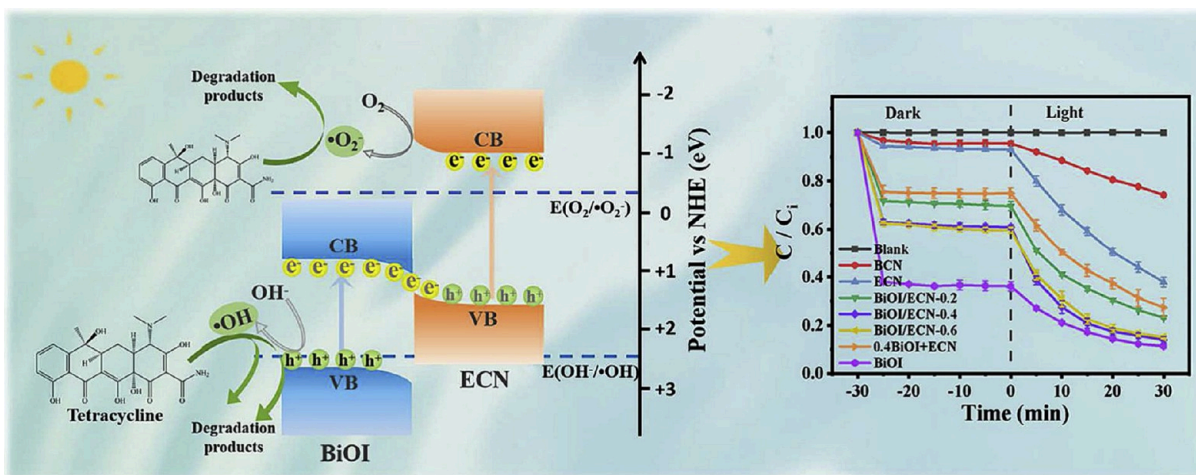
Figure 7. (a) Diagrams of the interfacial electron transfer between BiOI and ECN, (b) the degradation efficiency of RhB using all samples. Adapted in part with permission from ref 147. Copyright 2021 Elsevier.

Table 2. BBZSH Photocatalysts for the Removal of Antibiotics from Contaminated Water

S.No.	Photocatalysts	Synthesis methods	Application	Light source	Irradiation time (min)	Eff. (%)	ref.
1	MT-BiVO$_4$/g-C$_3$N$_4$	Hydrothermal method	Photocatalytic degradation of tetracycline hydrochloride from water				82
2	g-C$_3$N$_4$/Bi$_2$MoO$_6$/CeO$_2$	Facile solid-state thermolysis	Photocatalytic degradation of 4-chlomjnfc		80	99.1	58
3	Bi$_2$MoO$_6$/UiO-66−NH$_2$	Facile solvothermal	Photocatalytic degradation of ofloxacin and ciprofloxacin		90	100, 96	90
4	Ag$_3$PO$_4$/Bi$_2$S$_3$/Bi$_2$O$_3$		Photocatalytic degradation of sulfamethazine and cloxacillin		90	98.06, 90.26	148
5	TiO$_2$/Bi$_2$O$_3$	Facile sol−gel	Photocatalytic degradation of tetracycline hydrochloride (TC)	visible light	60	80	21
6	Au@TiO$_2$/Bi$_2$WO$_6$	Sol−gel and hydrothermal method	Photocatalytic degradation of sulfamethoxazole and TC		75	96.9, 95	57
7	CuBi$_2$O$_4$/Bi$_2$Sn$_2$O$_7$/Sn$_2$O$_7$	In situ growth method	Photocatalytic degradation of TC			89.7	60
8	CdS/Bi$_3$O$_4$Cl simple hydrothermal	Photocatalytic degradation of CIP and TC	250 Xe lamp		120	84.2	149
9	BiOCl-Au-CdS	Step-wise decomposition method	Photocatalytic degradation of sulfadiazine antibiotics	300W Xe lamp	240	100	59
10	BiOCl/Bi−Bi$_2$O$_3$	One-step hydrothermal method	Photocatalytic degradation of RhB and TC	300W Xe lamp	60	90, 70	150
11	AgVO$_3$/Bi$_4$Ti$_3$O$_{12}$	Simple precipitation method	Photodegradation of tetracycline (TC)		60	57	151
12	BiOBr/Bi$_2$O$_4$	Coprecipitation method	Photodegradation of 4-chlorophenol (4-CP)				56
13	CoAl−LDH/Bi$_2$MoO$_6$	Simple hydrothermal method	Photocatalytic degradation of tetracycline and ciprofloxacin			85.98, 72.69	152
14	TiO$_2$(B)/BiOCl	Simple hydrothermal method	Photodegradation of TC		100	80	153
15	CdS/BiOBr	Solvothermal route	Photocatalytic degradation of norfloxacin and ciprofloxacin			100	54
16	SnS$_2$/Bi$_2$WO$_6$	Hydrothermal route	Photocatalytic degradation of tetracycline (TC) and ciprofloxacin (CIP)			97, 93	55
17	Bi$_2$MoO$_6$/TiO$_2$	Solvothermal-calcination process	Photocatalytic degradation of tetracycline hydrochloride		120	90.8	154
18	AgI/Bi$_2$WO$_6$	In situ precipitation method	Photocatalytic degradation of TC		60	93.05	155
19	Bi$_2$Fe$_4$O$_9$/Bi$_2$MoO$_6$	Facile one-pot solvothermal	Photocatalytic degradation of MB and TC		150, 180		156
20	Bi$_2$WO$_6$/g-C$_3$N$_4$ and Bi$_2$WO$_6$/TiO$_2$	Hydrothermal methods	Photocatalytic degradation of cefixime		135	94, 91	157
21	Bi@β-Bi$_2$O$_3$/g-C$_3$N$_4$	In situ deposition and oxidation	Photocatalytic degradation of 2,3-dihydroxynaphthalene		100	87	158
22	Bi$_2$S$_3$/Bi$_2$O$_2$CO$_3$	A simple chemical route	Degradation of antibiotics and organic compounds	Sunlight	61	89	121
23	ZnIn$_2$S$_4$/BiVO$_4$	Hydrothermal method	Photocatalytic mineralization of antibiotics		180	60	159

Furthermore, Liu et al. also synthesized a Z-scheme heterojunction of BiOI and exfoliated g-C$_3$N$_4$ to degrade tetracycline in wastewater.[147] They used a combination of thermal exfoliation and chemical precipitation to synthesize the compounds. The

researchers tested the Photocatalytic activities of different photocatalysts, including BCN, ECN, BiOI, and different ratios of BiOI in BiOI/ECN compounds. They found that the Z-scheme heterojunction of BiOI-0.4 and ECN-0.4 had the highest degradation rate compared with other photocatalysts, including BCN, with photocatalytic activity up to 10 times greater than that of BCN. The charge transfer pathways and the interface band alignment of the constructed Z-scheme of BiOI/ECN are shown in Figure 7a and b depicts the degradation efficiency of RhB by synthesized samples. Furthermore, BBSc photocatalysts for the removal of antibiotics from wastewater are summarized in Table 2.

Aromatic Compounds Degradation. Aromatic chemicals are the most common and enduring contaminants in the environment.[160] The degradation of aromatic compounds is a crucial process in environmental remediation, particularly water. These compounds are commonly found in industrial wastewater and can have harmful effects on both human health and the ecosystem. To address this issue, the widely reported methods is biological degradation methods.[160−162] Recently researchers have been investigating various photocatalytic methods for the degradation of aromatic compounds.[163,164] Particularly, BBZSH photocatalysts have shown promising results in the degradation of aromatic compounds. Huang et al. synthesized BiOI/Bi$_2$WO$_6$ layered heterojunction using hydrothermal method for degradation of phenol. The construction of Z- scheme heterojunction photocatalysts has significantly improved the photocatalytic ability of degrading phenol.[164] Lan et al. synthesized heterojunction photocatalysts in the Z-scheme Bi@β-Bi$_2$O$_3$/g-C$_3$N$_4$ using an in situ deposition and oxidation method for the degradation of 2,3-dihydroxynaphthalene. The results of the study show that a heterojunction photocatalyst of the Z scheme was degraded with a removal ratio of 870% after 100 min of irradiation.[158] The efficient charge separation and enhanced photocatalytic activity of Z- scheme heterojunctions enable the effective degradation of these compounds into harmless byproducts. Furthermore, in the recent year a Z-scheme heterojunction of BiOBr/ZIF-8/ZnO photocatalyst was prepared for the removal of phenols in wastewater. The result demonstrates that the ideal BiOBr/ZIF-8/ZnO photocatalysts were shown to have the degradation efficiency of 90% of the removal of phenol or bisphenol in 2 h, with kinetic constants that were 3.8 and 2.3 times higher, respectively, than those of pure BiOBr.[165]

Endocrine-Disrupting Compound Degradation. It is believed that the endocrine system in the body is regulated by hormones through the endocrine system. Endocrine disrupting chemicals (EDCs) are synthetic or natural chemicals that can mimic, inhibit, or otherwise affect hormones. These chemicals are linked to numerous health problems.[166] Some sources of EDCs such as BPA, phythoetogens, pesticides, phthalates, dioxins, etc., are commonly found in water sources and can have detrimental effects on aquatic ecosystems and human health.[167] Bi-based heterojunction photocatalysts can help in the degradation of EDCs, breaking down their complex molecular structures and reducing their concentrations in contaminated water. For instance, a combined hydrothermal-calcination method was used to synthesize Z-scheme heterojunctions of P-doped g-3N$_4$/α-Bi$_2$O$_3$ nanocomposites for degrading refractory endocrine disruptors-benzophenones.[168] According to these studies, 25 wt % P-g-C$_3$N$_4$/α-Bi$_2$O$_3$ nanocomposite demonstrated superior degradation capability for 4-hydroxybenzophenone (4H-BP) and benzophenone-1. In a study by Li

et al. they prepared an AgI/BiOBr heterojunction using a chemical bath deposition method. The photocatalytic performance of synthesized photocatalysts was checked with the degradation of 17α-ethinylestradiol (EE2). 97.0% of the compound EE2 was eliminated within 9 min following irradiation. Compared to pure photocatalysts, AgI/BiOBr heterojunctions have 16.0 and 138.7 times more rate constant than pure AgI and BiOBr, respectively.[169] Bi/γ-Bi$_2$O$_3$/O-doped g-C$_3$N$_4$ heterojunction photocatalysts was synthesized using solvothermal method for degradation of bisphenol A (BPA). It has been shown that Bi/γ-Bi$_2$O$_3$/EtCN heterojunctions are more active in photocatalytic degradation of bisphenol A (BPA) than g-C$_3$N$_4$ and ethanol assisted carbon nitride (EtCN), with a degradation rate 15.67 times higher than g-C$_3$N$_4$. The catalyst exhibits a broad light absorption range due to the all-solid heterojunction formed between Bi$_2$O$_3$ and EtCN with Bi acting as an electron shuttle as shown in Figure 8.[170]
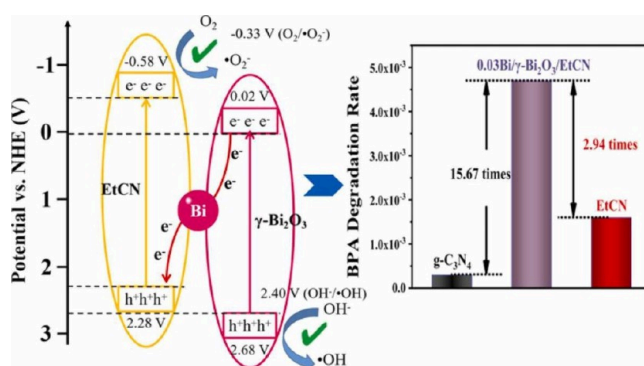
Figure 8. Schematic diagram of Z-scheme heterojunction of Bi/γ-Bi$_2$O$_3$/EtCN and its BPA degradation rate. Adapted in part with permission from ref 170 .Copyright 2022 Elsevier.

Volatile Organic Compound (VOC) Degradation. Chemicals known as volatile organic compounds (VOCs) are frequently released from the burning of fuels, industrial production of waste gases, and the use of decorative paints and photochemical pollution.[171−173] Among VOs, toluene threatens the ecosystem and human life. Hence, several methods such as adsorption, biofiltration, and thermal catalysis have been used for removal of toluene from environment.[171] Nevertheless, those approaches have drawbacks, such as low efficiency and large energy requirements. Therefore, recent research indicates that photocatalytic oxidation is an effective method for removing VOCs from the environment. The Z-scheme heterojunction photocatalysts based on Bi have demonstrated potential for degrading VOCs via photocatalytic oxidation. For example, Shi et al. synthesized a ternary Z-scheme heterojunction BiVO$_4$/BiPO$_4$/g-C$_3$N$_4$ photocatalyst and high-specific surface area semicoke activated carbon (SAC) for degradation of volatile organic compounds. The surface area of the prepared semicoke activated carbon is 619.27 m^2 g^1. Under simulated sunshine irradiation, the composite of BiVO$_4$/BiPO$_4$/g-C$_3$N$_4$/SAC degrades toluene by 85.6% in 130 min, which is 2.43 times that of pure photocatalyst.[173] Recently, Xu et al. prepared Bi$_2$O$_3$ quantum dots deco- rated TiO$_2$/BiOBr dual Z-scheme heterojunction photocatalysts for degradation of gaseous toluene.[172] These studies result shows that, the presences of Bi$_2$O$_3$ quantum dots and BiOBr in the photocatalysts were regulated and the optimized removal rate for gaseous toluene. In a recent study reported by Guo et al. heterojunction of Bi$_2$WO$_6$/
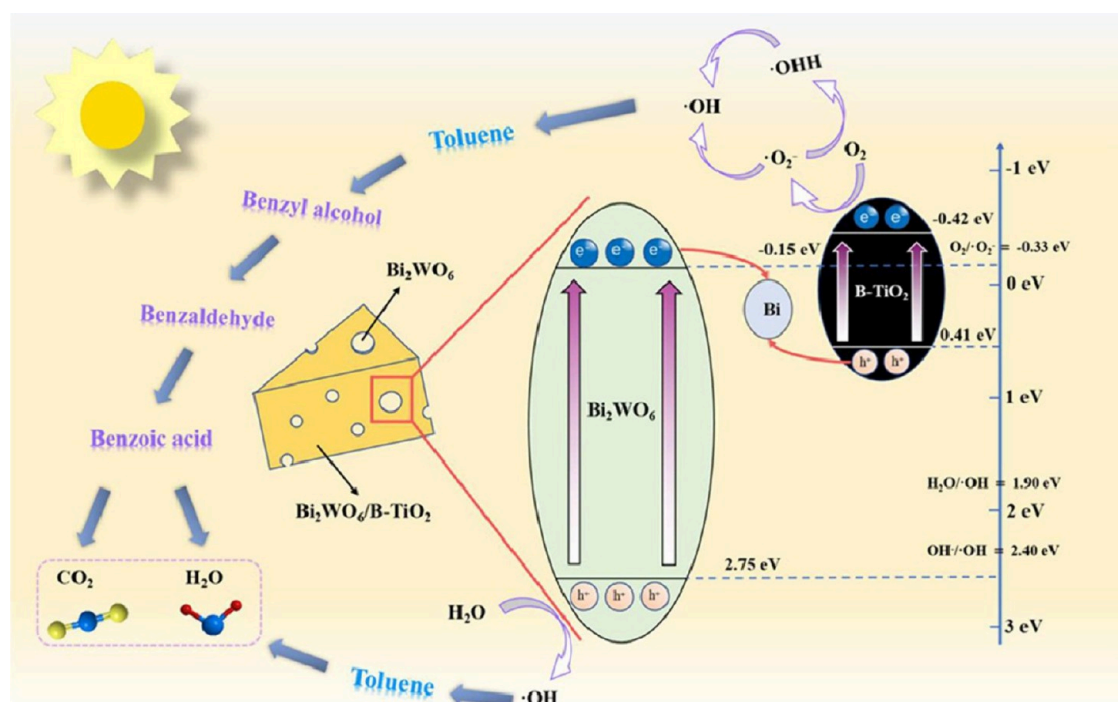
Figure 9. Mechanism of toluene degradation using the Z-scheme heterojunction of Bi_2WO_6/black-TiO_2 photocatalysts. Adapted in part with permission from ref 174. Copyright 2023 Elsevier.

black-TiO_2 photocatalysts for degradation of toluene was synthesized by using a combination of hydrothermal and sol−gel methods. The heterojunction of Bi_2WO_6/black-TiO_2 photocatalysts exhibits the best photocatalytic activity of converting 90% of toluene after 120 min, which is twice that of B-TiO_2 and 55 times that of Bi_2WO_6.[174] The mechanism of toluene degradation is shown in Figure 9. Recently Jia et al. synthesized a direct Z-scheme of WO_3/Bi_2WO_6 using a simple hydrothermal process for degradation of toluene.[171] The studies result demonstrates that, the highest rate of photocatalytic toluene conversion (92%) in 60 min, whereas the pure WO_3 (45%) and Bi_2WO_6 (63%).

Conclusion, Challenges, and Future Prospective. Over the last three decades, attempts have been made to tackle the serious planetary problems using different techniques such as biodegradation, advanced oxidation processes (AOPs) (e.g., catalysis, photo-Fenton oxidation, Fenton-like oxidation, and electrochemical oxidation process adsorption), filtration, and adsorption methods. However, most of these methods are expensive. This remains because of subtle hazardous pollutants. However, photocatalysis- based water treatment is considered to be a green technology because it is cost-effective and environmentally friendly. Owing to their unique layered structure and the internal electric fields between the layers, chemical stability, availability, and affordability, BBSc photo-catalysts have received attention in photocatalytic applications for water treatment. Furthermore, compared to other metal oxide photocatalysts, BBSc has better photocatalytic efficiency owing to the hybrid orbitals in the valence band and the absorption of broad visible-light radiation. BBSc photocatalysts can be prepared using chemicals such as solvothermal/ hydrothermal, coprecipitation, chemical bath deposition, solution combustion, etc., physical methods include ball milling, physical vapor deposition, and green synthesis methods.

While pure BBSc photocatalysts are more efficient than other metal oxide photocatalysts, they have some limitations, including a narrow visible light absorption range, high recombination rate, and low redox capacity, all of which affect their catalytic activity. Researchers have recently been working extensively to improve BBSc photocatalysts using various methods. In particular, the construction of heterojunctions and elemental doping have been widely utilized to overcome their drawbacks. Based on the VB and CB edge locations of the two coupled semiconductors, three types of heterojunctions can be constructed (type I, type II, and type III). There are three charge transfer mechanism are sensitization, Type-II and Z-scheme. Sensitization involves using a sensitizer to extend the light absorption range of a photocatalyst. Type II hetero-junctions have staggered energy band alignments, enabling efficient charge separation and transfer. Z-scheme hetero-junctions involve the transfer of electrons and holes between two photocatalysts, facilitating a continuous redox cycle and enhancing photocatalytic efficiency.

Generally speaking, the photocatalytic degradation mecha-nism involves the absorption of light, charge separation, transfer of electrons and holes between photocatalysts, and sub- sequent redox reactions. The Z-scheme design enhances charge separation and minimizes recombination, resulting in improved photocatalytic degradation efficiency. It is crucial to note that the efficiency of photoinduced charge transfer in heterojunction photocatalysts depends on various factors, including the energy band alignment, morphology, surface area, and interfacial charge transfer kinetics. Proper selection and design of the hetero-junction materials are crucial for optimizing the charge transfer process and maximizing photocatalytic activity. The charge transfer mechanism in the Z-scheme and S-scheme is similar to that in the type II heterojunction, but the main difference is the way electron−hole formation. In a Z-scheme heterojunction, an electron hole is created by the sequential excitation of two

coupled photocatalysts. The S-scheme heterojunction was created by simultaneous excitation of the two photocatalysts. Additionally, charge transfer occurs because of the Fermi energy difference in the S-scheme heterojunction, which facilitates more charge separation during the catalysis process. Despite their great potential for removing pollutants and antibiotics from contaminated water, Z-scheme heterojunction photocatalysts also have some challenges.[175]

- One of the key challenges is selecting suitable materials for both the electron donor and acceptor in the Z-scheme photocatalysts. Finding materials with compatible band gaps and suitable band alignment is critical but can be a complex task.[176]

- The separation and transfer of charge carriers across the heterojunction interfaces must be fast and efficient to minimize recombination losses. Designing the heterojunction architecture and optimizing the surface area and crystallinity of the materials can help improve charge transfer.

- Ensuring the long-term stability and durability of Z-scheme heterojunction photocatalysts. Many photocatalysts may experience degradation or structural changes over time due to factors like photocorrosion, harsh reaction conditions, or surface passivation. Developing catalysts with high resistance to photocorrosion and maintaining the stability of the junctions under operational conditions are other challenges.

- Achieving high-performance photocatalysts at a large scale and reasonable cost is a challenge. Some materials used in Z-scheme photocatalysts, such as noble metals or rare earth elements, can be expensive or scarce. Therefore, developing cost-effective and abundant alternatives is crucial for their widespread implementation.

- Understanding the reaction kinetics and optimizing parameters to enhance selectivity toward the desired products is an ongoing challenge. This involves detailed characterization techniques, computational modeling, and optimization of reaction conditions.

To tackle these difficulties, it is necessary to bring together experts from different fields such as materials science, chemistry, physics, and engineering. If these obstacles can be overcome, Z-scheme heterojunction photocatalysts can be more efficient, reliable, and cost-effective, making them suitable for use in the production of clean energy and the remediation of the environment. The outlook for Z-scheme heterojunction photocatalysts is very encouraging, as they provide several benefits and potential for further growth and utilization.

- Future research efforts will likely focus on developing new S-scheme heterojunction systems with optimized band alignments and improved interfacial charge transfer to achieve higher photocatalytic activity.

- Further exploration of S-scheme heterojunction systems in different photocatalytic applications such as solar energy conversion, environmental remediation, water splitting, pollutant degradation, CO_2 reduction, and sustainable chemistry. Researchers can explore diverse material combinations to tailor the band alignments and optimize the charge transfer pathways. This opens up opportunities for discovering new materials and designing high-performance S-scheme heterojunction photocatalysts.

- Exploring the synergistic effects between the S-scheme configuration and cocatalysts or cocatalytic reactions can lead to improved catalytic performance and increased reaction selectivity. Integrating cocatalysts or cocatalytic reactions with S-scheme heterojunctions offers a versatile approach to enhance their catalytic performance. By promoting charge separation, facilitating surface reactions, and creating synergistic effects, cocatalysts effectively improve the overall efficiency and effectiveness of S-scheme heterojunction photocatalysts.[116]

- Future research efforts will likely focus on deepening our understanding of the charge transfer dynamics, interfacial phenomena, and reaction kinetics involved in S-scheme systems. This fundamental knowledge will guide the rational design and optimization of S-scheme heterojunctions for enhanced photocatalytic activity.

- Future research will address the development of scalable and economically viable synthesis methods, as well as the integration of S-scheme heterojunction photocatalysts into practical devices and systems. The scalability and economic viability of synthesis methods for S-scheme heterojunction photocatalysts can be improved in several ways such as the following:[109]

  - To reduce time, energy, and resource consumption, identify critical reaction parameters, such as temperature, pressure, and catalyst concentration, and optimizing them for improved efficiency and scalability.

  - To produce high yield catalysts, choose synthesis methods that yield high product yields, which is crucial for economic viability. Designing environmentally friendly synthesis methods is essential for sustainability and cost-effectiveness.

  - Exploring cost-effective and readily available precursors and raw materials can significantly impact the economic viability of the synthesis methods.

  - Another strategy is collaboration between researchers and industrial partners, as well as the sharing of knowledge and best practices, which can accelerate the development of scalable and economically viable synthesis methods.

- Future research will address the development of scalable and economically viable synthesis methods, as well as the integration of S-scheme heterojunction photocatalysts into practical devices and systems. The practical implementation of S-scheme heterojunction photocatalysts in real-world devices and systems presents both challenges and opportunities.[177]

  - Some challenges are (i) scalability, (ii) stability and durability, (iii) cost-effectiveness, and (iv) reactant selectivity and specificity.

  - Some potential opportunities are (i) enhanced photocatalytic activity, (ii) extended light absorption range, and (iii) stability and durability compared to single component photocatalysts

Generally, to realize these opportunities in practical applications, further research and development are required to optimize the synthesis methods, enhance the stability, and improve the scalability of S-scheme heterojunction photocatalysts.

In conclusion, the future of S-scheme heterojunction photocatalysts holds considerable potential for advancing the field of photocatalysis. Their enhanced photocatalytic activity, a broader range of applications, material combinations, integration of cocatalysts, and fundamental understanding will drive further developments and pave the way for their practical implementation in various fields. Integrating cocatalysts or cocatalytic reactions with S-scheme heterojunctions helps in promoting charge separation, facilitating surface reactions, and creating synergistic effects. Continued research and exploration in this area will undoubtedly contribute to the advancement of sustainable and clean energy technologies.

■ AUTHOR INFORMATION

Corresponding Author

Abebe Belay Gemta − *Department of Applied Physics, Adama Science and Technology University, Adama 1888, Ethiopia*; Phone: +251911712766; Email: abebebelay96@gmail.com

Authors

Tadesse Lemma Wakjira − *Department of Applied Physics, Adama Science and Technology University, Adama 1888, Ethiopia;* ⊙ orcid.org/0000-0002-3461-0195

Gashaw Beyene Kassahun − *Department of Applied Physics, Adama Science and Technology University, Adama 1888, Ethiopia*

Dinsefa Mensur Andoshe − *Department of Material Engineering, Adama Science and Technology University, Adama 1888, Ethiopia;* ⊙ orcid.org/0000-0001-9664-1344

Kumneger Tadele − *Department of Applied Physics, Adama Science and Technology University, Adama 1888, Ethiopia*

Complete contact information is available at:
https://pubs.acs.org/10.1021/acsomega.3c08939

Author Contributions

The following writers certify their contributions to the paper: **Tadesse Lemma Wakjira:** Conception, Draft manuscript writing, and Compilation of the final version. **Abebe Belay Gemta:** Conception, editing, and approval of the manuscript. **Gashaw Beyene Kassahun:** Conception and Editing. **Dinsefa Mensur Andoshe:** Formatting and Editing. **Kumneger Tadele:** Formatting and Editing.

Notes

The authors declare no competing financial interest.

■ REFERENCES

(1) Sarker, B.; Keya, K. N.; Mahir, F. I.; Nahiun, K. M.; Shahida, S.; Khan, R. A. Surface and ground water pollution: causes and effects of urbanization and industrialization in South Asia. *Scientific Review* **2021**, *7*, 32−41.

(2) Zakharov, S. V.; Lushpey, V. P.; Abbasova, L. R.; Zhongkai, S. Analysis of the im- pact of the energy industry on the environment. *IOP Conference Series: Earth and Environmental Science* **2022**, *1070*, 012044.

(3) Mohamed, E. F. Nanotechnology: future of environmental air pollution control. *Environmental Management and Sustainable Development* **2017**, *6*, 429.

(4) Bao, Y.; Chen, K. Novel Z-scheme BiOBr/reduced graphene oxide/protonated g-C3N4 photocatalyst: synthesis, characterization, visible light photocatalytic activity and mechanism. *Appl. Surf. Sci.* **2018**, *437*, 51−61.

(5) Fuller, R.; Landrigan, P. J.; Balakrishnan, K.; Bathan, G.; Bose-O'Reilly, S.; Brauer, M.; Caravanos, J.; Chiles, T.; Cohen, A.; Corra, L. Pollution and health: a progress update. *Lancet Planetary Health* **2022**, *6* (6), E535−E547.

(6) Guo, D.; Wang, H.; Fu, P.; Huang, Y.; Liu, Y.; Lv, W.; Wang, F. Diatomite precoat filtration for wastewater treatment: Filtration performance and pollution mechanisms. *Chem. Eng. Res. Des.* **2018**, *137*, 403−411.

(7) Aneyo, I. A.; Doherty, F. V.; Adebesin, O. A.; Hammed, M. O. Biodegradation of pollutants in waste water from pharmaceutical, textile and local dye effluent in Lagos, Nigeria. *Journal of Health and Pollution* **2016**, *6*, 34−42.

(8) Ngambia, A.; Ifthikar, J.; Shahib, I. I.; Jawad, A.; Shahzad, A.; Zhao, M.; Wang, J.; Chen, Z.; Chen, Z. Adsorptive purification of heavy metal contaminated wastewater with sewage sludge derived carbon-supported Mg (II) composite. *Sci. Total Environ.* **2019**, *691*, 306−321.

(9) Martı́nez-Huitle, C. A.; Panizza, M. Electrochemical oxidation of organic pollutants for wastewater treatment. *Current Opinion in Electrochemistry* **2018**, *11*, 62−71.

(10) Bauer, R.; Fallmann, H. The photo-Fenton oxidation—a cheap and efficient wastewater treatment method. *Research on chemical intermediates* **1997**, *23*, 341−354.

(11) Ebrahiem, E. E.; Al-Maghrabi, M. N.; Mobarki, A. R. Removal of organic pollutants from industrial wastewater by applying photo-Fenton oxidation technology. *Arabian Journal of Chemistry* **2017**, *10*, S1674−S1679.

(12) Lupu, G.-I.; Orbeci, C.; Bobirică, L.; Bobirică, C.; Pascu, L. F. Key Principles of Advanced Oxidation Processes: A Systematic Analysis of Current and Future Per- spectives of the Removal of Antibiotics from Wastewater. *Catalysts* **2023**, *13*, 1280.

(13) Baaloudj, O.; Kenfoud, H.; Badawi, A. K.; Assadi, A. A.; El Jery, A.; Assadi, A. A.; Amrane, A. Bismuth sillenite crystals as recent photocatalysts for water treatment and energy generation: A critical review. *Catalysts* **2022**, *12*, 500.

(14) Kumar, S.; Ahlawat, W.; Bhanjana, G.; Heydarifard, S.; Nazhad, M. M.; Dilbaghi, N. Nanotechnology-based water treatment strategies. *Journal of nanoscience and nan- otechnology* **2014**, *14*, 1838−1858.

(15) Zhao, B.; Shao, N.; Chen, X.; Ma, J.; Gao, Y.; Chen, X. Construction of novel type II heterojunction WO₃/Bi₂WO₆ and Z-scheme heterojunction CdS/Bi₂WO₆ photo- catalysts with significantly enhanced photocatalytic activity for the degradation of rhodamine B and reduction of Cr (VI). *Colloids Surf., A* **2023**, *663*, 131072.

(16) Zheng, X.; Song, Y.; Liu, Y.; Yang, Y.; Wu, D.; Yang, Y.; Feng, S.; Li, J.; Liu, W.; Shen, Y.; Tian, X. ZnIn₂S₄-based photocatalysts for photocatalytic hydrogen evolution via water splitting. *Coord. Chem. Rev.* **2023**, *475*, 214898.

(17) Yang, Y.; Zheng, X.; Song, Y.; Liu, Y.; Wu, D.; Li, J.; Liu, W.; Fu, L.; Shen, Y.; Tian, X. CuInS2-based photocatalysts for photocatalytic hydrogen evolution via water splitting. *Int. J. Hydrogen Energy* **2023**, *48*, 3791−3806.

(18) Sayed, M.; Yu, J.; Liu, G.; Jaroniec, M. Non-noble plasmonic metal-based photocatalysts. *Chem. Rev.* **2022**, *122*, 10484−10537.

(19) Mubeen, K.; Irshad, A.; Safeen, A.; Aziz, U.; Safeen, K.; Ghani, T.; Khan, K.; Ali, Z.; ul Haq, I.; Shah, A. Band structure tuning of ZnO/CuO composites for enhanced photocatalytic activity. *Journal of Saudi Chemical Society* **2023**, *27*, 101639.

(20) Wang, Q.; Chen, K.; Wang, S.; Jiang, D.; Ma, C.; Zhu, L.; Xu, X. An in situ-fabricated p-Co₃O₄@n-ZnO surface heterojunction photocatalyst for solar-to-fuel conversion of CO₂. *Materials Chemistry Frontiers* **2023**, *7*, 523.

(21) Xie, Z.; Wang, W.; Ke, X.; Cai, X.; Chen, X.; Wang, S.; Lin, W.; Wang, X. A heptazine-based polymer photocatalyst with donor-acceptor configuration to promote exciton dissociation and charge separation. *Applied Catalysis B: Environmental* **2023**, *325*, 122312.

(22) Zhang, Y.-J.; Cheng, J.-Z.; Xing, Y.-Q.; Tan, Z.-R.; Liao, G.; Liu, S.-Y. Solvent- exfoliated DA π-polymer@ZnS heterojunction for efficient photocatalytic hydrogen evolution. *Materials Science in Semiconductor Processing* **2023**, *161*, 107463.

(23) Tharuman, S.; Balakumar, V.; Vinodhini, J.; Karthikeyani, R.; Mayandi, J.; Sasirekha, V.; Pearce, J. Visible light driven photocatalytic performance of 3D TiO₂/g-C₃N₄ nanocomposite via Z-scheme charge transfer promotion for water purification. *J. Mol. Liq.* **2023**, *371*, 121101.

(24) Zahraei, M. S. N.; Fazaeli, R.; Aliyan, H.; Richeson, D. Photocatalytic degradation abilities of binary core-shell SiO₂@ mZrO₂/TiO₂ nanocomposites: Characterization, kinetic and thermo-dynamic study of metoclopramide (MCP) eradication for water purification. *Mater. Res. Bull.* **2023**, *157*, 112029.

(25) Hazaraimi, M.; Goh, P.; Lau, W.; Ismail, A.; Wu, Z.; Subramaniam, M.; Lim, J.; Kanakaraju, D. The state-of-the-art development of photocatalysts for degrading of persistent herbicides in aqueous environment. *Sci. Total Environ.* **2022**, *843*, 156975.

(26) Zhang, L.; Li, Y.; Li, Q.; Fan, J.; Carabineiro, S. A.; Lv, K. Recent advances on Bismuth-based Photocatalysts: Strategies and mecha-nisms. *Chemical Engineering Journal* **2021**, *419*, 129484.

(27) Cao, S.; Zhou, P.; Yu, J. Recent advances in visible light Bi-based photocatalysts. *Chinese Journal of Catalysis* **2014**, *35*, 989−1007.

(28) Meng, X.; Zhang, Z. Bismuth-based photocatalytic semi-conductors: introduction, challenges and possible approaches. *J. Mol. Catal. A: Chem.* **2016**, *423*, 533−549.

(29) Wang, S.; Wang, L.; Huang, W. Bismuth-based photocatalysts for solar energy con- version. *Journal of materials chemistry A* **2020**, *8*, 24307−24352.

(30) Wang, R.; Li, H.; Sun, H. Bismuth: environmental pollution and health effects. *Encyclopedia of environmental health* **2019**, 415.

(31) Chen, Y.; Zhou, Y.; Zhang, J.; Li, J.; Yao, T.; Chen, A.; Xiang, M.; Li, Q.; Chen, Z.; Zhou, Y. Plasmonic Bi promotes the construction of Z-scheme heterojunction for efficient oxygen molecule activation. *Chemosphere* **2022**, *302*, 134527.

(32) Iyyapushpam, S.; Nishanthi, S.; Padiyan, D. P. Synthesis of β-Bi₂O₃ towards the application of photocatalytic degradation of methyl orange and its instability. *J. Phys. Chem. Solids* **2015**, *81*, 74−78.

(33) Zhao, G.-q.; Zheng, Y.-j.; He, Z.-g.; Lu, Z.-x.; Wang, L.; Li, C.-f.; Jiao, F.-p.; Deng, C.-y. Synthesis of Bi₂S₃ microsphere and its efficient photocatalytic activity under visible- light irradiation. *Transactions of Nonferrous Metals Society of China* **2018**, *28*, 2002−2010.

(34) Yao, B.; Zheng, G.; Luan, Y.; Wang, L.; Xing, X.; Wang, Y.; Liu, Y.; He, J.; Zhang, F. Cost-effective Bi₂WO₆ for efficient degradation of rhodamine B and tetracycline. *Journal of Materials Science: Materials in Electronics* **2023**, *34*, 246.

(35) Ji, T.; Ha, E.; Wu, M.; Hu, X.; Wang, J.; Sun, Y.; Li, S.; Hu, J. Controllable hydrothermal synthesis and photocatalytic performance of Bi₂MoO₆ nano/microstructures. *Catalysts* **2020**, *10*, 1161.

(36) Jin, X.; Zhong, J.; Zhang, S. Ionic liquids assisted preparation of BiPO₄ photocata- lyst with enhanced photocatalytic activity for tetracycline and rhodamine B removal. *Environmental Technology* **2023**, *44*, 2669−2678.

(37) Wu, L.; Yue, X.; Chang, Y.; Wang, K.; Zhang, J.; Sun, J.; Wei, Z.; Kowalska, E. Photocatalytic Degradation of Tetracycline under Visible Light Irradiation on BiVO₄ Microballs Modified with Noble Metals. *Catalysts* **2022**, *12*, 1293.

(38) Subhiksha, V.; Kokilavani, S.; Sudheer Khan, S. Recent advances in degradation of organic pollutant in aqueous solutions using bismuth based photocatalysts: A review. *Chemo- sphere* **2022**, *290*, 133228.

(39) Monny, S. A.; Wang, Z.; Konarova, M.; Wang, L. Bismuth based photoelectrodes for solar water splitting. *Journal of Energy Chemistry* **2021**, *61*, 517−530.

(40) Li, J.; Yuan, H.; Zhang, W.; Jin, B.; Feng, Q.; Huang, J.; Jiao, Z. Advances in Z- scheme semiconductor photocatalysts for the photoelectrochemical applications: A review. *Carbon Energy* **2022**, *4*, 294−331.

(41) Li, H.; Jian, L.; Chen, Y.; Wang, G.; Lyu, J.; Dong, X.; Liu, X.; Ma, H. Fabricating Bi₂MoO₆@Co₃O₄ core-shell heterogeneous architec-tures with Z-scheme for superior photoelectrocatalytic water purification. *Chemical Engineering Journal* **2022**, *427*, 131716.

(42) He, X.; Kai, T.; Ding, P. Heterojunction photocatalysts for degradation of the tetra- cycline antibiotic: a review. *Environmental Chemistry Letters* **2021**, *19*, 4563−4601.

(43) Jia, T.; Wu, J.; Xiao, Y.; Liu, Q.; Wu, Q.; Qi, Y.; Qi, X. Self-grown oxygen vacancies- rich CeO₂/BiOBr Z-scheme heterojunction decorated with rGO as charge transfer channel for enhanced

photocatalytic oxidation of elemental mercury. *J. Colloid Interface Sci.* **2021**, *587*, 402−416.

(44) Kato, D.; Hongo, K.; Maezono, R.; Higashi, M.; Kunioku, H.; Yabuuchi, M.; Suzuki, H.; Okajima, H.; Zhong, C.; Nakano, K.; et al. Valence band engineering of layered bismuth oxyhalides toward stable visible-light water splitting: Madelung site potential analysis. *J. Am. Chem. Soc.* **2017**, *139*, 18725−18731.

(45) Che, H.; Liu, C.; Hu, W.; Hu, H.; Li, J.; Dou, J.; Shi, W.; Li, C.; Dong, H. NGQD active sites as effective collectors of charge carriers for improving the photocatalytic performance of Z-scheme g-C₃N₄/Bi₂WO₆ heterojunctions. *Catalysis Science & Technology* **2018**, *8*, 622−631.

(46) Huang, L.; Liu, J.; Li, Y.; Yang, L.; Wang, C.; Liu, J.; Li, H.; Huang, L. Enhancement of photocatalytic activity of Z-scheme BiO₂₋ₓ/BiOI heterojunction through vacancy engineering. *Appl. Surf. Sci.* **2021**, *555*, 149665.

(47) Wang, B.; Zhao, J.; Chen, H.; Weng, Y.-X.; Tang, H.; Chen, Z.; Zhu, W.; She, Y.; Xia, J.; Li, H. Unique Z-scheme carbonized polymer dots/Bi₄O₅Br₂ hybrids for efficiently boosting photocatalytic CO₂ reduction. *Applied Catalysis B: Environmental* **2021**, *293*, 120182.

(48) Wei, J.; Chen, Z.; Tong, Z. Engineering Z-scheme silver oxide/bismuth tungstate heterostructure incorporated reduced graphene oxide with superior visible-light photocatalytic activity. *J. Colloid Interface Sci.* **2021**, *596*, 22−33.

(49) Chen, F.; Yang, Q.; Wang, Y.; Yao, F.; Ma, Y.; Huang, X.; Li, X.; Wang, D.; Zeng, G.; Yu, H. Efficient construction of bismuth vanadate-based Z-scheme photocatalyst for simultaneous Cr (VI) reduction and ciprofloxacin oxidation under visible light: Kinetics, degradation pathways and mechanism. *Chemical Engineering Journal* **2018**, *348*, 157−170.

(50) Stelo, F.; Kublik, N.; Ullah, S.; Wender, H. Recent advances in Bi₂MoO₆ based Z-scheme heterojunctions for photocatalytic degrada-tion of pollutants. *J. Alloys Compd.* **2020**, *829*, 154591.

(51) Raja, A.; Rajasekaran, P.; Vishnu, B.; Selvakumar, K.; Teon Do, J.; Swaminathan, M.; Kang, M. Fabrication of effective visible-light-driven ternary Z-scheme ZnO-Ag-BiVO₄ heterostructured photocatalyst for hexavalent chromium reduction. *Sep. Purif. Technol.* **2020**, *252*, 117446.

(52) Wang, C.; Li, S.; Cai, M.; Yan, R.; Dong, K.; Zhang, J.; Liu, Y. Rationally de- signed tetra (4-carboxyphenyl) porphyrin/graphene quantum dots/bismuth molyb- date Z-scheme heterojunction for tetracycline degradation and Cr (VI) reduction: Performance, mechanism, intermediate toxicity appraisement. *J. Colloid Interface Sci.* **2022**, *619*, 307−321.

(53) Li, X.; Yang, K.; Wang, F.; Shi, K.; Huang, W.; Lu, K.; Yu, C.; Liu, X.; Zhou, M. Constructing 0D/1D Bi2S3/Sb2S3 Z-scheme hetero-junctions for efficient visible-light- driven degradation of dyes, Cr⁶⁺ reduction and H₂O₂ production. *J. Alloys Compd.* **2023**, *953*, 170064.

(54) Senasu, T.; Nijpanich, S.; Juabrum, S.; Chanlek, N.; Nanan, S. CdS/BiOBr heterojunction photocatalyst with high performance for solar-light-driven degradation of ciprofloxacin and norfloxacin anti-biotics. *Appl. Surf. Sci.* **2021**, *567*, 150850.

(55) Kumar, G.; Dutta, R. K. Fabrication of plate-on-plate SnS₂/Bi₂WO₆ nanocomposite as photocatalyst for sunlight mediated degradation of antibiotics in aqueous medium. *J. Phys. Chem. Solids* **2022**, *164*, 110639.

(56) Yang, R.; Qin, F.; Zheng, S.; Hu, C.; Ma, Y.; Liang, B.; Bai, Y.; Zhang, C. Fabrication of three-dimensional hierarchical BiOBr/Bi₂O₄ p-n heterojunction with excellent visible light photodegradation performance for 4-chlorophenol. *J. Phys. Chem. Solids* **2022**, *161*, 110381.

(57) Jin, K.; Qin, M.; Li, X.; Wang, R.; Zhao, Y.; Wang, H. Z-scheme Au@TiO₂/Bi₂WO₆ heterojunction as efficient visible-light photo-catalyst for degradation of antibiotics. *J. Mol. Liq.* **2022**, *364*, 120017.

(58) Gao, Q.; Wang, Z.; Li, J.; Liu, B.; Liu, C. Facile synthesis of ternary dual Z- scheme g-C₃N₄/Bi₂MoO₆/CeO₂ photocatalyst with enhanced 4-chlorophenol removal: Degradation pathways and mechanism. *Environ. Pollut.* **2022**, *315*, 120436.

(59) Li, Q.; Guan, Z.; Wu, D.; Zhao, X.; Bao, S.; Tian, B.; Zhang, J. Z-scheme BiOCl-Au-CdS heterostructure with enhanced sunlight-driven

photocatalytic activity in degrading water dyes and antibiotics. *ACS Sustainable Chem. Eng.* 2017, 5, 6958−6968.

(60) Xu, J.; Zhu, Y.; Liu, Z.; Teng, X.; Gao, H.; Zhao, Y.; Chen, M. Synthesis of Dual Z-Scheme CuBi2O4/Bi2Sn2O7/Sn3O4 Photo-catalysts with Enhanced Photocatalytic Performance for the Degradation of Tetracycline under Visible Light Irradiation. *Catalysts* 2023, 13, 1028.

(61) Mohan, R.; Leonard, N.; Wieland, L. Applications of bismuth (III) compounds in organic synthesis. *Tetrahedron* 2002, 58, 8373−8397.

(62) Wu, S.; Xu, Z.; Zhang, J.; Zhu, M. Recent Progress on Metallic Bismuth-Based Photocatalysts: Synthesis, Construction, and Application in Water Purification. *Solar Rrl* 2021, 5, 2100668.

(63) Gujar, T.; Shinde, V.; Lokhande, C.; Mane, R.; Han, S.-H. Bismuth oxide thin films prepared by chemical bath deposition (CBD) method: annealing effect. *Appl. Surf. Sci.* 2005, 250, 161−167.

(64) Guan, H.; Zhang, X.; Xie, Y. Soft-chemical synthetic non-stoichiometric Bi2O2. 33 nanoflower: a new room-temperature ferromagnetic semiconductor. *J. Phys. Chem. C* 2014, 118, 27170−27174.

(65) Jain, A.; Ong, S. P.; Hautier, G.; Chen, W.; Richards, W. D.; Dacek, S.; Cholia, S.; Gunter, D.; Skinner, D.; Ceder, G.; Persson, K. A. Commentary: The Materials Project: A materials genome approach to accelerating materials innovation. *APL Materials* 2013, 1, 011002.

(66) Ajiboye, T. O.; Onwudiwe, D. C. Bismuth sulfide based compounds: Properties, syn- thesis and applications. *Results in Chemistry* 2021, 3, 100151.

(67) Collu, D. A.; Carucci, C.; Piludu, M.; Parsons, D. F.; Salis, A. Aurivillius oxides nanosheets-based photocatalysts for efficient oxidation of malachite green dye. *Inter- national Journal of Molecular Sciences* 2022, 23, 5422.

(68) Wei, Z.; Liu, J.; Fang, W.; Qin, Z.; Jiang, Z.; Shangguan, W. Enhanced photocatalytic hydrogen evolution using a novel in situ heterojunction yttrium-doped Bi4NbO8Cl@ Nb2O5. *Int. J. Hydrogen Energy* 2018, 43, 14281−14292.

(69) Xu, K.; Wang, L.; Xu, X.; Dou, S. X.; Hao, W.; Du, Y. Two dimensional bismuth-based layered materials for energy-related applications. *Energy Storage Materials* 2019, 19, 446−463.

(70) Chen, J.; Gu, Y.; Xu, S.; Zhang, Y.; Zhang, Z.; Shi, L.; Mu, Z.; Zhou, C.; Zhang, J.; Zhang, Q. Band Gap Engineering in Quadruple-Layered Sillen-Aurivillius Perovskite Oxychlorides Bi7Fe2Ti2O17X (X= Cl, Br, I) for Enhanced Photocatalytic Perfor- mance. *Catalysts* 2023, 13, 751.

(71) Bard, A. J. Photoelectrochemistry and heterogeneous photo-catalysis at semiconduc- tors. *J. Photochem.* 1979, 10, 59−75.

(72) Miseki, Y.; Fujiyoshi, S.; Gunji, T.; Sayama, K. Photocatalytic water splitting under visible light utilizing I^{3-}/I^- and IO^{3-}/I^- redox mediators by Z-scheme system using surface treated PtO_x/WO_3 as O_2 evolution photocatalyst. *Catalysis Science & Technology* 2013, 3, 1750−1756.

(73) Sayama, K.; Yoshida, R.; Kusama, H.; Okabe, K.; Abe, Y.; Arakawa, H. Photocatalytic decomposition of water into H_2 and O_2 by a two-step photoexcitation reaction using a WO_3 suspension catalyst and an Fe^{3+}/Fe^{2+} redox system. *Chem. Phys. Lett.* 1997, 277, 387−391.

(74) Sasaki, Y.; Kato, H.; Kudo, A. [Co (bpy) 3]$^{3+/2+}$ and [Co (phen) 3]$^{3+/2+}$ electron mediators for overall water splitting under sunlight irradiation using Z-scheme photo- catalyst system. *J. Am. Chem. Soc.* 2013, 135, 5441−5449.

(75) Tada, H.; Mitsui, T.; Kiyonaga, T.; Akita, T.; Tanaka, K. All-solid-state Z-scheme in CdS-Au-TiO2 three-component nanojunction system. *Nature materials* 2006, 5, 782−786.

(76) Jiang, R.; Lu, G.; Yan, Z.; Wu, D.; Zhou, R.; Bao, X. Insights into a CQD- SnNb2O6/BiOCl Z-scheme system for the degradation of benzocaine: Influence fac- tors, intermediate toxicity and photocatalytic mechanism. *Chemical Engineering Jour- nal* 2019, 374, 79−90.

(77) Zhang, T.; Wang, Y.; Xie, X.; Shao, Y.; Zeng, Y.; Zhang, S.; Yan, Q.; Li, Z. Dual Z-scheme 2D/3D carbon-bridging modified g-C3N4/BiOI-Bi2O3 composite photocatalysts for effective boosting visible-light-driven photocatalytic performance. *Sep. Purif. Technol.* 2021, 277, 119443.

(78) Zhang, M.; Yin, H.-f; Yao, J.-c.; Arif, M.; Qiu, B.; Li, P.-f.; Liu, X.-h. All-solid-state Z-scheme BiOX (Cl, Br)-Au-CdS heterostructure: Photocatalytic activity and degradation pathway. *Colloids Surf., A* 2020, 602, 124778.

(79) Chen, F.; Yang, Q.; Li, X.; Zeng, G.; Wang, D.; Niu, C.; Zhao, J.; An, H.; Xie, T.; Deng, Y. Hierarchical assembly of graphene-bridged Ag3PO4/Ag/BiVO4 (040) Z- scheme photocatalyst: an efficient, sustainable and heterogeneous catalyst with enhanced visible-light photoactivity towards tetracycline degradation under visible light irradiation. *Applied Catalysis B: Environmental* 2017, 200, 330−342.

(80) Ng, B.-J.; Putri, L. K.; Kong, X. Y.; Teh, Y. W.; Pasbakhsh, P.; Chai, S.-P. Z-scheme photocatalytic systems for solar water splitting. *Advanced science* 2020, 7, 1903171.

(81) Schumacher, L.; Marschall, R. Recent Advances in Semi-conductor Heterojunctions and Z-Schemes for Photocatalytic Hydrogen Generation. *Topics in Current Chemistry* 2022, 380, 53.

(82) Yin, X.; Sun, X.; Mao, Y.; Wang, R.; Li, D.; Xie, W.; Liu, Z.; Liu, Z. Synergistically enhanced photocatalytic degradation of tetracycline hydrochloride by Z-scheme heterojunction MT-BiVO4 microsphere/ P-doped g-C3N4 nanosheet composite. *Journal of Environmental Chemical Engineering* 2023, 11, 109412.

(83) Abid, N.; Khan, A. M.; Shujait, S.; Chaudhary, K.; Ikram, M.; Imran, M.; Haider, J.; Khan, M.; Khan, Q.; Maqbool, M. Synthesis of nanomaterials using various top-down and bottom-up approaches, influencing factors, advantages, and disadvantages: A review. *Adv. Colloid Interface Sci.* 2022, 300, 102597.

(84) Pal, G.; Rai, P.; Pandey, A. *Green Synthesis, Characterization and Applications of Nanoparticles*; Elsevier, 2019; pp 1−26.

(85) Chong, D. S.; Foo, J. J.; Tan, X.-Q.; Ling, G. Z. S.; Tan, L.-L.; Chen, X.; Ong, W.-J. Evolutionary face-to-face 2D/2D bismuth-based heterojunction: The quest for sustainable photocatalytic applications. *Applied Materials Today* 2022, 29, 101636.

(86) Hu, M.; Yan, A.; Li, F.; Huang, F.; Huang, J.; Cui, Q.; Wang, X. Z-scheme indium sulfide/bismuth oxybromide heterojunctions with enhanced visible-light photodegradation of organics. *Appl. Surf. Sci.* 2021, 547, 149234.

(87) Li, Z.; Bao, Z.; Yao, F.; Cao, H.; Wang, J.; Qiu, L.; Lv, J.; Sun, X.; Zhang, Y.; Wu, Y. One-dimensional bismuth vanadate nanostructures constructed Z-scheme photocata- lyst for highly efficient degradation of antibiotics. *Journal of Water Process Engineering* 2022, 46, 102599.

(88) Xue, W.; Huang, D.; Li, J.; Zeng, G.; Deng, R.; Yang, Y.; Chen, S.; Li, Z.; Gong, X.; Li, B. others Assembly of AgI nanoparticles and ultrathin g-CN nanosheets codecorated BiWO direct dual Z-scheme photocatalyst: An efficient, sustainable and heterogeneous catalyst with enhanced photocatalytic performance. *Chem. Eng. J.* 2019, 373, 1144.

(89) Ni, Z.; Shen, Y.; Xu, L.; Xiang, G.; Chen, M.; Shen, N.; Li, K.; Ni, K. Facile con- struction of 3D hierarchical flower-like Ag2WO4/Bi2WO6 Z-scheme heterojunction photocatalyst with enhanced visible light photocatalytic activity. *Appl. Surf. Sci.* 2022, 576, 151868.

(90) Su, Q.; Li, J.; Wang, B.; Li, Y.; Hou, L. others Direct Z-scheme Bi2MoO6/UiO-66-NH2 heterojunctions for enhanced photocatalytic degradation of ofloxacin and ciprofloxacin under visible light. *Applied Catalysis B: Environmental* 2022, 318, 121820.

(91) Chou, X.; Ye, J.; He, J.; Ge, K.; Liu, J.; Fu, C.; Zhou, X.; Wang, S.; Zhang, Y.; Yang, Y. One-Step Solvothermal Synthesis of BiPO4/ Bi2MoO6 Heterostructure with Oxygen Vacancies and Z-Scheme System for Enhanced Photocatalytic Performance. *ChemistrySelect* 2019, 4, 8327−8333.

(92) Hezam, A.; Namratha, K.; Drmosh, Q. A.; Ponnamma, D.; Nagi Saeed, A. M.; Ganesh, V.; Neppolian, B.; Byrappa, K. Direct Z-scheme Cs 2 O-Bi 2 O 3-ZnO heterostructures for photocatalytic overall water splitting. *Journal of Materials Chemistry A* 2018, 6, 21379−21388.

(93) Sahnesarayi, M. K.; Rastegari, S.; Sarpoolaky, H. Enhanced photoelectrochemical water splitting performance of vertically aligned Bi2O3 nanosheet arrays derived from chemical bath deposition method by controlling chemical bath temperature and complexing agent concentration. *Surfaces and Interfaces* 2022, 30, 101819.

(94) Dutta, V.; Chauhan, A.; Verma, R.; Gopalkrishnan, C.; Nguyen, V.-H. Recent trends in Bi-based nanomaterials: challenges, fabrication, enhancement techniques, and environmental applications. *Beilstein Journal of Nanotechnology* **2022**, *13*, 1316−1336.

(95) Vahabirad, S.; Nezamzadeh-Ejhieh, A. Co-precipitation synthesis of BiOI/(BiO)$_2$CO$_3$: brief characterization and the kinetic study in the photodegradation and mineralization of sulfasalazine. *J. Solid State Chem.* **2022**, *310*, 123018.

(96) Hou, D.; Hu, X.; Hu, P.; Zhang, W.; Zhang, M.; Huang, Y. Bi$_4$Ti$_3$O$_{12}$ nanofibers- BiOI nanosheets p−n junction: facile synthesis and enhanced visible-light photocatalytic activity. *Nanoscale* **2013**, *5*, 9764−9772.

(97) Liu, L.; Li, Y.; Zhu, C.; Yang, N.; Li, Y.; Su, F.; Qian, J. Visible light-driven Z-scheme Bi$_2$O$_3$/CuBi$_2$O$_4$ heterojunction with dual metal ions cycle for PMS activation and Lev degradation. *Inorg. Chem. Commun.* **2023**, *158*, 111531.

(98) Shi, H.; Wei, X.; Zhang, J.; Long, Q.; Liu, W.; Zhou, Y.; Ding, Y. Green Synthesis and Direct Z-Scheme CdSe/BiOCl Heterojunctions for Enhanced Photocatalytic Performance. *ChemistrySelect* **2020**, *5*, 6230−6235.

(99) Li, J.; Lu, T.; Zhao, Z.; Xu, R.; Li, Y.; Huang, Y.; Yang, C.; Zhang, S.; Tang, Y. Preparation of heterostructured ternary Cd/CdS/BiOCl photocatalysts for enhanced visible-light photocatalytic degradation of organic pollutants in wastewater. *Inorg. Chem. Commun.* **2020**, *121*, 108236.

(100) Chen, P.; Liu, H.; Cui, W.; Lee, S. C.; Wang, L.; Dong, F. Bi-based photocatalysts for light-driven environmental and energy applications: structural tuning, reaction mechanisms, and challenges. *EcoMat* **2020**, *2*, No. e12047.

(101) Fan, H.; Ma, X.; Li, X.; Yang, L.; Bian, Y.; Li, W. Fabrication of Novel g-C3N4@ Bi/Bi$_2$O$_2$CO$_3$ Z-Scheme Heterojunction with Meliorated Light Absorption and Efficient Charge Separation for Superior Photocatalytic Performance. *Molecules* **2022**, *27*, 8336.

(102) Din, S. T. U.; Lee, H.; Yang, W. Z-scheme heterojunction of 3-dimensional hierarchical Bi$_3$O$_4$Cl/Bi$_5$O$_7$I for a significant enhancement in the photocatalytic degradation of organic pollutants (RhB and BPA). *Nanomaterials* **2022**, *12*, 767.

(103) Opoku, F.; Govender, K. K.; van Sittert, C. G. C. E.; Govender, P. P. Recent progress in the development of semiconductor-based photocatalyst materials for applications in photocatalytic water splitting and degradation of pollutants. *Advanced Sustainable Systems* **2017**, *1*, 1700006.

(104) Wang, J.; Wang, Z.; Dai, K.; Zhang, J. Review on inorganic-organic S-scheme photo- catalysts. *Journal of Materials Science & Technology* **2023**, *165*, 187.

(105) Shawky, A.; Mohamed, R. S-scheme heterojunctions: emerging designed photocatalysts toward green energy and environmental remediation redox reactions. *Journal of Environmental Chemical Engineering* **2022**, *10*, 108249.

(106) San Martín, S.; Rivero, M. J.; Ortiz, I. Unravelling the mechanisms that drive the performance of photocatalytic hydrogen production. *Catalysts* **2020**, *10*, 901.

(107) Bie, C.; Yu, J. Application of S-Scheme Heterojunction Photocatalyst. *UV-Visible Photocatalysis for Clean Energy Production and Pollution Remediation: Materials, Reaction Mechanisms, and Applications* **2023**, 41−58.

(108) Low, J.; Yu, J.; Jiang, C. *Interface Science and Technology*; Elsevier, 2020; Vol. *31*; pp 193−229.

(109) Odabasi Lee, S.; Lakhera, S. K.; Yong, K. Strategies to Enhance Interfacial Spatial Charge Separation for High-Efficiency Photocatalytic Overall Water-Splitting: A Re- view. *Advanced Energy and Sustainability Research* **2023**, *4*, 2300130.

(110) Ong, W.-J.; Tan, L.-L.; Ng, Y. H.; Yong, S.-T.; Chai, S.-P. Graphitic carbon nitride (g-C$_3$N$_4$)-based photocatalysts for artificial photosynthesis and environmental reme- diation: are we a step closer to achieving sustainability? *Chem. Rev.* **2016**, *116*, 7159−7329.

(111) Liu, W.-W.; Peng, R.-F. Recent advances of bismuth oxychloride photocatalytic material: Property, preparation and performance enhancement. *Journal of Electronic Science and Technology* **2020**, *18*, 100020.

(112) Liang, M.; Yang, Z.; Yang, Y.; Mei, Y.; Zhou, H.; Yang, S. One-step introduction of metallic Bi and non-metallic C in Bi$_2$WO$_6$ with enhanced photocatalytic activity. *Journal of Materials Science: Materials in Electronics* **2019**, *30*, 1310−1321.

(113) Belousov, A. S.; Parkhacheva, A. A.; Suleimanov, E. V.; Fukina, D. G.; Korya- gin, A. V.; Shafiq, I.; Krasheninnikova, O. V.; Kuzmichev, V. V. Doping vs. het- erojunction: A comparative study of the approaches for improving the photocatalytic activity of flower-like Bi$_2$WO$_6$ for water treatment with domestic LED light. *Catal. Commun.* **2023**, *180*, 106705.

(114) Hezam, A.; Peppel, T.; Strunk, J. Pathways towards a systematic development of Z scheme photocatalysts for CO2 reduction. *Current Opinion in Green and Sustainable Chemistry* **2023**, *41*, 100789.

(115) Chen, S.; Qi, Y.; Li, C.; Domen, K.; Zhang, F. Surface strategies for particulate photocatalysts toward artificial photosynthesis. *Joule* **2018**, *2*, 2260−2288.

(116) Zhang, L.; Zhang, J.; Yu, H.; Yu, J. Emerging S-scheme photocatalyst. *Advanced materials* **2022**, *34*, 2107668.

(117) Xu, Q.; Zhang, L.; Cheng, B.; Fan, J.; Yu, J. S-scheme heterojunction photocatalyst. *Chem.* **2020**, *6*, 1543−1559.

(118) Bie, C.; Zhang, L.; Yu, J. *Interface Science and Technology*; Elsevier, 2023; Vol. *35*; pp 253−287.

(119) Thakur, A.; Kumar, A. Recent advances on rapid detection and remediation of environmental pollutants utilizing nanomaterials-based (bio) sensors. *Science of The Total Environment* **2022**, *834*, 155219.

(120) Kumar, A.; Dixit, U.; Singh, K.; Gupta, S. P.; Beg, M. S. J. Structure and properties of dyes and pigments. *Dyes and Pigments-Novel Applications and Waste Treatment*; InTech Open, 2021; p 131.

(121) Bai, L.; Cao, Y.; Pan, X.; Shu, Y.; Dong, G.; Zhao, M.; Zhang, Z.; Wu, Y.; Wang, B. Z-scheme Bi$_2$S$_3$/Bi$_2$O$_2$CO$_3$ nanoheterojunction for the degradation of antibiotics and organic compounds in wastewater: Fabrication, application, and mechanism. *Surfaces and Interfaces* **2023**, *36*, 102612.

(122) Song, S.; Xing, Z.; Zhao, H.; Li, Z.; Zhou, W. Recent advances in bismuth-based photocatalysts: Environment and energy applications. *Green Energy & Environment* **2023**, *8*, 1232.

(123) Mosleh, S.; Dashtian, K.; Ghaedi, M.; Amiri, M. A Bi$_2$WO$_6$/Ag$_2$S/ZnS Z-scheme heterojunction photocatalyst with enhanced visible-light photoactivity towards the degradation of multiple dye pollutants. *RSC Adv.* **2019**, *9*, 30100−30111.

(124) Bi, H.; Liu, J.; Wu, Z.; Zhu, K.; Suo, H.; Lv, X.; Fu, Y.; Jian, R.; Sun, Z. Construction of Bi$_2$WO$_6$/ZnIn$_2$S$_4$ with Z-scheme structure for efficient photocatalytic performance. *Chem. Phys. Lett.* **2021**, *769*, 138449.

(125) Mahalakshmi, K.; Ranjith, R.; Thangavelu, P.; Priyadharshini, M.; Palanivel, B.; Manthrammel, M. A.; Shkir, M.; Diravidamani, B. Augmenting the Photocatalytic Performance of Direct Z-Scheme Bi$_2$O$_3$/g-C$_3$N$_4$ Nanocomposite. *Catalysts* **2022**, *12*, 1544.

(126) Bavani, T.; Madhavan, J.; Preeyanghaa, M.; Neppolian, B.; Murugesan, S. Construction of direct Z-scheme g-C$_3$N$_4$/BiYWO$_6$ heterojunction photocatalyst with enhanced visible light activity towards the degradation of methylene blue. *Environmental Science and Pollution Research* **2023**, *30*, 10179−10190.

(127) Zhong, K.; Feng, J.; Gao, H.; Zhang, Y.; Lai, K. Fabrication of BiVO$_4$@ g-C$_3$N$_4$ (100) heterojunction with enhanced photocatalytic visible-light-driven activity. *J. Solid State Chem.* **2019**, *274*, 142−151.

(128) Hao, H.; Lu, D.; Zhang, J. Fabrication of novel double Z-scheme photocatalyst WO$_3$-Ag$_3$PO$_4$-Bi$_2$WO$_6$ with excellent visible photo-catalytic activity. *Int. J. Environ. Chem.* **2018**, *2*, 56−66.

(129) Li, B.; Lai, C.; Zeng, G.; Qin, L.; Yi, H.; Huang, D.; Zhou, C.; Liu, X.; Cheng, M.; Xu, P.; et al. Facile hydrothermal synthesis of Z-scheme Bi$_2$Fe$_4$O$_9$/Bi$_2$WO$_6$ heterojunction photocatalyst with enhanced visible light photocatalytic activity. *ACS Appl. Mater. Interfaces* **2018**, *10*, 18824−18836.

(130) Cheng, Y.; Shah, N. H.; Yang, J.; Zhang, K.; Cui, Y.; Wang, Y. Bi-based Z-scheme nanomaterials for the photocatalytic degradation of organic dyes. *ACS Applied Nano Materials* **2019**, *2*, 6418−6427.

(131) Ge, L.; Han, C.; Liu, J. Novel visible light-induced g-C3N4/Bi2WO6 composite photocatalysts for efficient degradation of methyl orange. *Applied Catalysis B: Environ- mental* **2011**, *108*, 100−107.

(132) Fenelon, E.; Bui, D.-P.; Tran, H. H.; You, S.-J.; Wang, Y.-F.; Cao, T. M.; Van Pham, V. Straightforward synthesis of SnO2/Bi2S3/BiOCl-Bi24O31Cl10 composites for drastically enhancing rhodamine B photocatalytic degradation under visible light. *ACS omega* **2020**, *5*, 20438−20449.

(133) Yi, J.; Zeng, H.; Lin, H.; Li, M.; Xie, R.; Chen, B.; Ding, R.; Liu, Z.; Li, D.; Li, N. Fabrication of direct Z-scheme Ag_2O/Bi_2MoO_6 heterostructured microsphere with enhanced visible-light photo-catalytic activity. *J. Alloys Compd.* **2023**, *935*, 168151.

(134) Cao, J.; Zhao, Y.; Lin, H.; Xu, B.; Chen, S. Facile synthesis of novel Ag/AgI/BiOI composites with highly enhanced visible light photocatalytic performances. *J. Solid State Chem.* **2013**, *206*, 38−44.

(135) Li, J.; Yuan, H.; Zhu, Z. Fabrication of $Cu_2O/Au/BiPO_4$ Z-scheme photocatalyst to improve the photocatalytic activity under solar light. *J. Mol. Catal. A: Chem.* **2015**, *410*, 133−139.

(136) Lu, X.; Ma, X.; Li, Q.; Dai, K.; Zhang, J.; Zhang, M.; Cui, C.; Zhu, G.; Liang, C. Fabrication of $Ag_2O/KNbO_3$ heterojunction with high visible-light photocatalytic activity. *J. Nanopart. Res.* **2019**, *21*, 1−12.

(137) Li, J.; Yuan, H.; Zhu, Z. Improved photoelectrochemical performance of Z-scheme g- $C_3N_4/Bi_2O_3/BiPO_4$ heterostructure and degradation property. *Applied Surface Sci- ence* **2016**, *385*, 34−41.

(138) Sun, M.; Wang, Y.; Shao, Y.; He, Y.; Zeng, Q.; Liang, H.; Yan, T.; Du, B. Fabrication of a novel Z-scheme g-C3N4/Bi4O7 heterojunction photocatalyst with enhanced visible light-driven activity toward organic pollutants. *J. Colloid Interface Sci.* **2017**, *501*, 123−132.

(139) Sharma, S.; Ibhadon, A. O.; Francesconi, M. G.; Mehta, S. K.; Elumalai, S.; Kansal, S. K.; Umar, A.; Baskoutas, S. Bi_2WO_6/C-Dots/TiO2: a novel Z-scheme pho- tocatalyst for the degradation of fluoroquinolone levofloxacin from aqueous medium. *Nanomaterials* **2020**, *10*, 910.

(140) Lv, Y.-R.; Liu, C.-J.; He, R.-K.; Li, X.; Xu, Y.-H. $BiVO_4/TiO_2$ heterojunction with enhanced photocatalytic activities and photo-electochemistry performances under visible light illumination. *Mater. Res. Bull.* **2019**, *117*, 35−40.

(141) Drisya, K.; Solı́s-Lopez, M.; Rı́os-Ramı́rez, J.; Durán-Álvarez, J.; Rousseau, A.; Velumani, S.; Asomoza, R.; Kassiba, A.; Jantrania, A.; Castaneda, H. Electronic and optical competence of TiO2/BiVO4 nanocomposites in the photocatalytic processes. *Sci. Rep.* **2020**, *10*, 13507.

(142) Alahmadi, M.; Alsaedi, W. H.; Mohamed, W.; Hassan, H. M.; Ezzeldien, M.; Abu- Dief, A. M. Development of $Bi_2O_3/MoSe_2$ mixed nanostructures for photocatalytic degradation of methylene blue dye. *Journal of Taibah University for Science* **2023**, *17*, 2161333.

(143) Akbari, M. Z.; Xu, Y.; Lu, Z.; Peng, L. Review of antibiotics treatment by advance oxidation processes. *Environmental Advances* **2021**, *5*, 100111.

(144) Pan, Z.; Qian, L.; Shen, J.; Huang, J.; Guo, Y.; Zhang, Z. Construction and application of Z-scheme heterojunction In2O3/Bi4O7 with effective removal of antibiotic under visible light. *Chemical Engineering Journal* **2021**, *426*, 130385.

(145) Wen, X.-J.; Qian-Lu; Lv, X.-X.; Sun, J.; Guo, J.; Fei, Z.-H.; Niu, C.-G. Photocatalytic degradation of sulfamethazine using a direct Z-Scheme AgI/Bi4V2O11 photocatalyst: Mineralization activity, degrada-tion pathways and promoted charge separation mech- anism. *Journal of hazardous materials* **2020**, *385*, 121508.

(146) Yin, X.; Sun, X.; Li, D.; Xie, W.; Mao, Y.; Liu, Z.; Liu, Z. 2D/2D phosphorus-doped g-C3N4/Bi2WO6 direct Z-Scheme heterojunction photocatalytic system for Tetracycline Hydrochloride (TC-HCl) degradation. *International Journal of Environmental Research and Public Health* **2022**, *19*, 14935.

(147) Liu, H.; Huo, W.; Zhang, T. C.; Ouyang, L.; Yuan, S. Photocatalytic removal of tetracycline by a Z-scheme heterojunction of bismuth oxyiodide/exfoliated g-C3N4: performance, mechanism, and degradation pathway. *Materials Today Chemistry* **2022**, *23*, 100729.

(148) Shao, B.; Liu, X.; Liu, Z.; Zeng, G.; Liang, Q.; Liang, C.; Cheng, Y.; Zhang, W.; Liu, Y.; Gong, S. A novel double Z-scheme photocatalyst $Ag_3PO_4/Bi_2S_3/Bi_2O_3$ with enhanced visible-light photocatalytic per-formance for antibiotic degradation. *Chemical Engineering Journal* **2019**, *368*, 730−745.

(149) Che, H.; Che, G.; Jiang, E.; Liu, C.; Dong, H.; Li, C. A novel Z-Scheme CdS/Bi3O4Cl heterostructure for photocatalytic degradation of antibiotics: Mineralization activity, degradation pathways and mechanism insight. *Journal of the Taiwan Institute of Chemical Engineers* **2018**, *91*, 224−234.

(150) Wu, K.; Qin, Z.; Zhang, X.; Guo, R.; Ren, X.; Pu, X. Z-scheme BiOCl/Bi-Bi2O3 heterojunction with oxygen vacancy for excellent degradation performance of antibiotics and dyes. *J. Mater. Sci.* **2020**, *55*, 4017−4029.

(151) Chen, Y.; Zhou, Y.; Zhang, J.; Li, J.; Yao, T.; Chen, A.; Chen, Z. Ag bridged Z-scheme AgVO3/Bi4Ti3O12 heterojunction for enhanced antibiotic degradation. *J. Phys. Chem. Solids* **2022**, *161*, 110428.

(152) Wu, L.; Hu, J.; Sun, C.; Jiao, F. Construction of Z-scheme CoAl-LDH/Bi2MoO6 heterojunction for enhanced photocatalytic degrada-tion of antibiotics in natural water bodies. *Process Safety and Environmental Protection* **2022**, *168*, 1109−1119.

(153) Zou, X.; Li, C.; Wang, L.; Wang, W.; Bian, J.; Bai, H.; Meng, X. Enhanced visible- light photocatalytic degradation of tetracycline antibiotic by 0D/2D TiO2 (B)/BiOCl Z-scheme heterojunction: Performance, reaction pathways, and mechanism investiga- tion. *Appl. Surf. Sci.* **2023**, *630*, 157532.

(154) Yin, Z.; Qi, S.; Deng, S.; Xu, K.; Liu, Z.; Zhang, M.; Sun, Z. Bi_2MoO_6/TiO_2 heterojunction modified with Ag quantum dots: a novel photocatalyst for the efficient degradation of tetracycline hydrochloride. *J. Alloys Compd.* **2021**, *888*, 161582.

(155) Xue, W.; Peng, Z.; Huang, D.; Zeng, G.; Wen, X.; Deng, R.; Yang, Y.; Yan, X. In situ synthesis of visible-light-driven Z-scheme AgI/Bi2WO6 heterojunction photocatalysts with enhanced photocatalytic activity. *Ceram. Int.* **2019**, *45*, 6340−6349.

(156) Zhang, H.; Bian, H.; Zhang, H.; Xu, B.; Wang, C.; Zhang, L.; Li, D.; Wang, F. Magnetic Separable $Bi_2Fe_4O_9/Bi_2MoO_6$ Heterojunctions in Z-Scheme with Enhanced Visible-Light Photocatalytic Activity for Organic Pollutant Degradation. *Catal. Lett.* **2020**, *150*, 2464−2473.

(157) Gordanshekan, A.; Arabian, S.; Solaimany Nazar, A. R.; Farhadian, M.; Tangestaninejad, S. A comprehensive comparison of green $Bi_2WO_6/g-C_3N_4$ and Bi_2WO_6/TiO_2 S-scheme heterojunctions for photocatalytic adsorption/degradation of Cefixime: Artificial neu-ral network, degradation pathway, and toxicity estimation. *Chemical Engineering Journal* **2023**, *451*, 139067.

(158) Lan, Y.; Li, Z.; Li, D.; Xie, W.; Yan, G.; Guo, S. Visible-light responsive Z-scheme Bi@ β-Bi2O3/g-C3N4 heterojunction for efficient photocatalytic degradation of 2, 3- dihydroxynaphthalene. *Chemical Engineering Journal* **2020**, *392*, 123686.

(159) Yan, X.; Wang, B.; Zhao, J.; Liu, G.; Ji, M.; Zhang, X.; Chu, P. K.; Li, H.; Xia, J. Hierarchical columnar ZnIn2S4/BiVO4 Z-scheme heterojunctions with carrier highway boost photocatalytic mineraliza-tion of antibiotics. *Chemical Engineering Journal* **2023**, *452*, 139271.

(160) Seo, J.-S.; Keum, Y.-S.; Li, Q. X. Bacterial degradation of aromatic compounds. *International journal of environmental research and public health* **2009**, *6*, 278−309.

(161) Fuchs, G.; Boll, M.; Heider, J. Microbial degradation of aromatic compounds—from one strategy to four. *Nature Reviews Microbiology* **2011**, *9*, 803−816.

(162) Dı́az, E.; Jı́menez, J. I.; Nogales, J. Aerobic degradation of aromatic compounds. *Curr. Opin. Biotechnol.* **2013**, *24*, 431−442.

(163) Torres-Pinto, A.; Sampaio, M. J.; Silva, C. G.; Faria, J. L.; Silva, A. M. Metal- free carbon nitride photocatalysis with in situ hydrogen peroxide generation for the degradation of aromatic compounds. *Applied Catalysis B: Environmental* **2019**, *252*, 128−137.

(164) Huang, X.; Guo, Q.; Yan, B.; Liu, H.; Chen, K.; Wei, S.; Wu, Y.; Wang, L. Study on photocatalytic degradation of phenol by BiOI/Bi2WO6 layered heterojunction synthesized by hydrothermal method. *J. Mol. Liq.* **2021**, *322*, 114965.

(165) Han, X.; Zhang, T.; Cui, Y.; Wang, Z.; Dong, R.; Wu, Y.; Du, C.; Chen, R.; Yu, C.; Feng, J.; et al. A bifunctional BiOBr/ZIF-8/ZnO photocatalyst with rich oxygen vacancy for enhanced wastewater treatment and H_2O_2 generation. *Molecules* **2023**, *28*, 2422.

(166) Zlatnik, M. G. Endocrine-disrupting chemicals and reproductive health. *Journal of midwifery & women's health* **2016**, *61*, 442−455.

(167) Fernández, M. F.; Román, M.; Arrebola, J. P.; Olea, N. Endocrine disruptors: time to act. *Current Environmental Health Reports* **2014**, *1*, 325−332.

(168) Berekute, A. K.; Yu, K.-P.; Chuang, Y.-H.; Lin, K.-Y. Novel visible-light-induced P- doped g-C3N4/α-Bi$_2$O$_3$ nanocomposite photocatalysts for enhanced degradation of refractory endocrine disruptors—benzophenones. *Appl. Surf. Sci.* **2023**, *607*, 154987.

(169) Li, L.; Li, H.; Long, Y.; Wang, S.; Chen, Y.; Zhang, S.; Wang, L.; Luo, L.; Jiang, F. Facile Synthesis of Flower-Like AgI/BiOBr Z-Scheme Nanocomposite with Enhanced Photocatalytic Activity for Degradation of 17 α-Estradiol (EE2). *Nano* **2019**, *14*, 1950007.

(170) Lu, S.; Wu, T.; Liu, Y.; Luo, H.; Jiang, F.; Nie, X.; Chen, H. All-solid Z-scheme Bi/γ-Bi$_2$O$_3$/O-doped g-C$_3$N$_4$ heterojunction with Bi as electron shuttle for visible-light photocatalysis. *J. Alloys Compd.* **2022**, *911*, 164980.

(171) Jia, Y.; Zhang, X.; Wang, R.; Yuan, J.; Zheng, R.; Zhang, J.; Qian, F.; Chen, Y.; Zhang, M.; Guo, L. Energy band engineering of WO$_3$/Bi$_2$WO$_6$ direct Z-scheme for enhanced photocatalytic toluene degradation. *Appl. Surf. Sci.* **2023**, *618*, 156636.

(172) Xu, H.; Yang, J.; Li, Y.; Fu, F.; Da, K.; Cao, S.; Chen, W.; Fan, X. Fabrication of Bi$_2$O$_3$ QDs decorated TiO$_2$/BiOBr dual Z-scheme photocatalysts for efficient degra- dation of gaseous toluene under visible-light. *J. Alloys Compd.* **2023**, *950*, 169959.

(173) Shi, L.; Xue, J.; Xiao, W.; Wang, P.; Long, M.; Bi, Q. Efficient degradation of VOCs using semi-coke activated carbon loaded ternary Z-scheme heterojunction photocatalyst BiVO$_4$-BiPO$_4$-gC$_3$N$_4$ under visible light irradiation. *Phys. Chem. Chem. Phys.* **2022**, *24*, 22987−22997.

(174) Guo, L.; Zhang, J.; Zhang, X.; Wang, R.; Jia, Y.; Long, H. Energy band matching Bi2WO$_6$/black-TiO$_2$ Z-scheme heterostructure for the enhanced visible-light photo- catalytic degradation of toluene. *Molecular Catalysis* **2023**, *550*, 113603.

(175) Wang, L.; Bie, C.; Yu, J. Challenges of Z-scheme photocatalytic mechanisms. *Trends in Chemistry* **2022**, *4*, 973.

(176) Nie, C.; Wang, X.; Lu, P.; Zhu, Y.; Li, X.; Tang, H. Advancements in S-scheme hetero- junction materials for photocatalytic environmental remediation. *Journal of Materials Science & Technology* **2024**, *169*, 182.

(177) Dharani, S.; Vadivel, S.; Gnanasekaran, L.; Rajendran, S. S-scheme heterojunction photocatalysts for hydrogen production: Current progress and future prospects. *Fuel* **2023**, *349*, 128688.